Published OnlineFirst November 11, 2011; DOI: 10.1158/0008-5472.CAN-11-1403

32. Tomida S, Takeuchi T, Shimada Y, Arima C, Matsuo K, Mitsudomi T, et al. Relapse-related molecular signature in lung adenocarcinomas identifies patients with dismal prognosis. J Clin Oncol 2009;27:2793–9.
33. Endele S, Rosenberger G, Geider K, Popp B, Tamer C, Stefanova I, et al. Mutations in GRIN2A and GRIN2B encoding regulatory subunits of NMDA receptors cause variable neurodevelopmental phenotypes. Nat Genet 2010;42:1021–6.
34. Wei X, Walia V, Lin JC, Teer JK, Prickett TD, Gartner J, et al. Exome sequencing identifies GRIN2A as frequently mutated in melanoma. Nat Genet 2011;43:442–6.
35. Kanehira M, Harada Y, Takata R, Shuin T, Miki T, Fujioka T, et al. Involvement of upregulation of DEPDC1 (DEP domain containing 1) in bladder carcinogenesis. Oncogene 2007;26:6448–55.
36. Harada Y, Kanehira M, Fujisawa Y, Takata R, Shuin T, Miki T, et al. Cell-permeable peptide DEPDC1-ZNF224 interferes with transcriptional repression and oncogenicity in bladder cancer cells. Cancer Res 2010; 70:5829–39.
37. Kretschmer C, Sterner-Kock A, Siedentopf F, Schoenegg W, Schlag PM, Kemmner W. Identification of early molecular markers for breast cancer. Mol Cancer 2011;10:15.

Published OnlineFirst November 11, 2011; DOI: 10.1158/0008-5472.CAN-11-1403

AACR American Association for Cancer Research

Cancer Research

The Journal of Cancer Research (1916–1930) | The American Journal of Cancer (1931–1940)

Identification of Genes Upregulated in *ALK*-Positive and *EGFR/KRAS/ALK*-Negative Lung Adenocarcinomas

Hirokazu Okayama, Takashi Kohno, Yuko Ishii, et al.

Cancer Res 2012;72:100-111. Published OnlineFirst November 11, 2011.

MCB
Journals.ASM.org

Regulatory Nexus of Synthesis and Degradation Deciphers Cellular Nrf2 Expression Levels

Takafumi Suzuki,[a] Tatsuhiro Shibata,[b] Kai Takaya,[a] Kouya Shiraishi,[c] Takashi Kohno,[c] Hideo Kunitoh,[d] Koji Tsuta,[e] Koh Furuta,[e] Koichi Goto,[f] Fumie Hosoda,[b] Hiromi Sakamoto,[g] Hozumi Motohashi,[h] Masayuki Yamamoto[a,i]

Department of Medical Biochemistry[a] and Center for Radioisotope Sciences,[h] Tohoku University Graduate School of Medicine, and Tohoku Medical-Megabank Organization,[i] Sendai, Japan; Divisions of Cancer Genomics,[b] Genome Biology,[c] and Genetics,[g] National Cancer Center Research Institute, and Divisions of Pathology and Clinical Laboratories, National Cancer Center Hospital,[e] Tokyo, Japan; Department of Respiratory Medicine, Mitsui Memorial Hospital, Tokyo, Japan[d]; Division of Thoracic Oncology, National Cancer Center Hospital East, Kashiwa City, Chiba, Japan[f]

Transcription factor Nrf2 (NF-E2-related factor 2) is essential for oxidative and electrophilic stress responses. While it has been well characterized that Nrf2 activity is tightly regulated at the protein level through proteasomal degradation via Keap1 (Kelch-like ECH-associated protein 1)-mediated ubiquitination, not much attention has been paid to the supply side of Nrf2, especially regulation of *Nrf2* gene transcription. Here we report that manipulation of *Nrf2* transcription is effective in changing the final Nrf2 protein level and activity of cellular defense against oxidative stress even in the presence of Keap1 and under efficient Nrf2 degradation, determined using genetically engineered mouse models. In excellent agreement with this finding, we found that minor A/A homozygotes of a single nucleotide polymorphism (SNP) in the human *NRF2* upstream promoter region (rs6721961) exhibited significantly diminished *NRF2* gene expression and, consequently, an increased risk of lung cancer, especially those who had ever smoked. Our results support the notion that in addition to control over proteasomal degradation and derepression from degradation/repression, the transcriptional level of the *Nrf2* gene acts as another important regulatory point to define cellular Nrf2 levels. These results thus verify the critical importance of human SNPs that influence the levels of transcription of the *NRF2* gene for future personalized medicine.

The *Nrf2* (NF-E2-related factor 2; or *Nfe2l2*) gene encodes a basic leucine zipper-type transcription factor that belongs to the CNC (cap'n'collar) family (1). Nrf2 displays its transactivation activity through dimerization with one of the small Maf (sMaf) proteins, and the Nrf2-sMaf heterodimer recognizes a specific DNA sequence known as the antioxidant (ARE)/electrophile response element (EpRE) (2, 3). Downstream target genes of Nrf2 include enzymes that act in detoxifying and antioxidative stress responses, enzymes related to glutathione synthesis, and transporters, which together constitute a network to facilitate the cellular adaptation to oxidative and xenobiotic stresses (4, 43). Studies with the *Nrf2* gene knockout ($Nrf2^{-/-}$) mouse clearly demonstrate that Nrf2 deficiency attenuates the response to oxidative and electrophilic stresses (5, 6), resulting in high-level susceptibility to a variety of toxic chemicals and carcinogens (7–9). Similarly, Nrf2-deficient mice are prone to the initiation of carcinogenesis, demonstrating that Nrf2 contributes to cancer chemoprevention (10–12). Conversely, large numbers of cancer cells express high levels of Nrf2, and this fact indicates that cancer cells hijack and exploit Nrf2 activity for their malignant growth (13–15).

One of the important characteristics of Nrf2 is the inducible nature of its function in response to oxidative and electrophilic stresses (16). Under homeostatic and stress-free conditions, cellular Nrf2 abundance is maintained at a very low level, as the ubiquitin E3 ligase complex composed of Keap1 (Kelch-like ECH-associated protein 1) and cullin 3 specifically promotes ubiquitination and proteasomal degradation of Nrf2 (16, 44). Notably, Keap1 acts as a sensor for electrophilic and oxidative stresses by using reactive cysteine residues within the protein (17). Exposure to electrophiles or reactive oxygen species hampers Keap1 activity, reducing Nrf2 ubiquitination and leading to the stabilization and nuclear translocation/accumulation of Nrf2 (17). Subsequently, the expression of a battery of Nrf2 target genes is induced for cytoprotection against these insults. Thus, cellular Nrf2 activity is induced by a derepression mechanism utilizing the proteasomal protein degradation machinery (4).

Multiple lines of evidence support the mechanism of Nrf2 derepression from proteasomal degradation, which accounts for the inducible expression of Nrf2 target genes. On the contrary, changes in the supply side of Nrf2 seem to be less significant under these stress conditions than the derepression/accumulation mechanism of the Nrf2 protein (18). Thus, not much attention has been paid to the contribution of transcriptional regulation of the *Nrf2* gene to the accumulation of Nrf2 protein and inducible expression of its target genes. However, several lines of evidence suggest the importance of the transcriptional regulation of the *Nrf2* gene. For instance, the *Nrf2* mRNA level was found to increase approximately 2-fold 6 h after treatment of an electrophile in murine keratinocytes (19).

A promoter single nucleotide polymorphism (SNP) of the mouse *Nrf2* gene was found to be tightly linked to the sensitivity/

Received 16 January 2013 Returned for modification 31 January 2013
Accepted 1 April 2013
Published ahead of print 9 April 2013
Address correspondence to Masayuki Yamamoto, masiyamamoto@med.tohoku.ac.jp.
Takafumi Suzuki and Tatsuhiro Shibata contributed equally to this article.
Supplemental material for this article may be found at http://dx.doi.org/10.1128/MCB.00065-13.

doi:10.1128/MCB.00065-13

resistance of various inbred mouse lines to the toxicity of high concentrations (95%) of oxygen (8). Similarly, a variant of the *NRF2* gene in the upstream promoter region (rs6721961) (20) is associated with susceptibility to acute lung injury in humans (21). This human SNP is located in the middle of the ARE motif and weakens the affinity of NRF2 binding to the ARE. This regulatory SNP (rSNP) appears to disrupt the positive-feedback regulation of *NRF2* expression by NRF2 itself (21). Other consequences of this *NRF2* rSNP have also been reported, including the risk of venous thromboembolism (22), reduced vital capacity (23), and an impaired forearm vasodilator response (24).

However, it remains to be determined how significantly the *Nrf2* transcript level affects Nrf2 definitive activity *in vivo*. This is the most critical issue for the future use of this and related *NRF2* SNPs in risk assessment and personalized medicine. Therefore, to address this critical issue, we have exploited genetically engineered mouse models. Our present results unequivocally demonstrate the importance of the level of the Nrf2 supply in both the presence and absence of Keap1-mediated protein degradation regulation. In addition, in order to clarify how significantly the reduction of the *NRF2* mRNA level is linked to the pathogenesis of human diseases, we explored whether the *NRF2* rSNP rs6721961 contributes to the increased risk of non-small-cell lung carcinomas. We compared the incidence of each genotype of the *NRF2* rSNP in a lung cancer population and a control population. We also measured the endogenous expression of *NRF2* in immortalized lymphocytes. We found that the rSNP genotype indeed affects the *NRF2* mRNA level in peripheral lymphocytes and also brings about an increased risk of non-small-cell lung cancers. These results strongly argue that transcription of the *NRF2* gene is an important regulatory point for cellular NRF2 activity.

MATERIALS AND METHODS

Mice. *Nrf2*$^{-/-}$ and Keap1 gene knockout (*Keap1*$^{-/-}$) mice were produced and characterized as described previously (6, 25). Transgene construct *KRD*-Nrf2 was generated by subcloning the Flag-hemagglutinin (HA)-tagged mouse Nrf2 cDNA into the vector harboring a 5.7-kb *Keap1* gene regulatory domain (*KRD*) (26). Transgenic mice were generated as described previously (26). Four independent lines were established for *KRD*-Nrf2. All compound mutant mice examined in this study were from a mixed genetic background, with contributions from 129Sv/J, C57BL/6J, and ICR strains. For hematoxylin-eosin (H&E) staining, the esophagi of P10 pups or adult mice were fixed in 3.7% formalin and embedded in paraffin.

Cell culture. Peritoneal macrophages were isolated as described previously (5). Whole-cell extracts were prepared in a lysis buffer (26) and subjected to immunoblot analysis using anti-Nrf2 (27), anti-Flag (Sigma-Aldrich), anti-HA (Roche), and anti-α-tubulin (Sigma-Aldrich) antibodies. Cell viability after 1-chloro-2,4-dinitrobenzene (CDNB) treatment was determined using a Cell Counting Kit-8 (Dojin Laboratories) according to the manufacturer's protocol. Diethyl maleate (DEM) and CDNB were purchased from Wako Pure Chemicals. Menadione and benzyl isothiocyanate (BITC) were purchased from Sigma-Aldrich.

Real-time PCR. Total RNA was prepared from forestomachs or macrophages using an Isogen RNA extraction kit (Nippon Gene) or from immortalized lymphocytes using an RNeasy kit (Qiagen). The cDNAs were synthesized from the total RNA using SuperScript III reverse transcriptase (Invitrogen by Life Technology). Real-time quantitative PCR was performed using an ABI 7300 (Applied Biosystems by Life Technology) or LightCycler 480 (Roche) system. Primer and probe sequences are available upon request.

Study participants. All lung cancer cases and controls were Japanese. These cases received treatments at the National Cancer Center Hospitals (NCCH), Japan, from 2000 to 2008. All surgically collected lung cancer specimens were pathologically examined by at least two board-certified pathologists in the NCCH. Histological diagnosis is based on the WHO classification of lung tumors (28). The controls were volunteers enrolled at the NCCH and at Keio University, located in Tokyo, Japan, with the following inclusion criteria: they could not have lung or other cancers or a history of cancer. All cases and controls, all of whom provided informed consent, were consecutively included in this study without any exclusion criteria. This study was approved by the institutional review boards of the National Cancer Center. Smoking habit was expressed by the number of pack-years, which was defined as the number of cigarette packs smoked daily multiplied by the number of years of smoking. Those who had never smoked (never smokers) were defined as individuals for whom the number of pack-years was 0. Those who had ever smoked (ever smokers) were defined as individuals for whom the number of pack-years was >0 and included both former and current smokers.

SNP analysis. Genomic DNA was extracted from whole blood from lung cancer cases and controls enrolled in the NCCH. Genomic DNA was extracted from Epstein-Barr virus-transformed B lymphocytes derived from whole blood collected from volunteers enrolled at Keio University. Genomic DNA was extracted using a blood maxikit or a QIAamp DNA minikit (Qiagen). The genotypes of NRF2 rSNP rs6721961 (referred to here as NRF2 rSNP-617) were determined by TaqMan SNP genotyping assays (Applied Biosystems by Life Technology).

Detection of somatic *EGFR* and *KRAS* mutations in lung tumors. Tumor samples were obtained at the time of surgery, rapidly frozen in liquid nitrogen, and stored at −80°C. Genomic DNA from the tissues was extracted using a QIAamp DNA minikit (Qiagen). Somatic mutations in the *EGFR* and *KRAS* genes were examined by high-resolution melting analysis (HRMA) as previously described (29).

Statistical analysis. Odds ratios (ORs) and 95% confidence intervals (CIs) for lung adenocarcinoma (ADC) risk were calculated after adjusting for gender, age (≤49, 50 to 59, 60 to 69, and ≥70 years), and smoking (never smoker versus ever smoker) by unconditional logistic regression analysis. These analyses were performed using JMP (version 8.0) software (SAS Institute Inc., Cary, NC).

RESULTS

Reflection of *Nrf2* gene dosage on cellular Nrf2 activity. To clarify how significantly reduction of *Nrf2* synthesis affects Nrf2 activity *in vivo*, we decided to exploit genetically engineered mouse models and examine whether transcriptional regulation of the *Nrf2* gene makes a substantial contribution to Nrf2 activity. Because Keap1 represses Nrf2 activity by accelerating the proteasomal degradation of the Nrf2 protein, a *Keap1*-null background provides an ideal model to analyze the gene dosage effect of *Nrf2*. Importantly, in this model system we can ignore the influence of Nrf2 degradation provoked by the Keap1-based ubiquitination of Nrf2. Indeed, *Keap1* gene knockout results in the constitutive accumulation of Nrf2, and the *Keap1*-null background is lethal in pups due to severe hyperkeratosis of the upper digestive tract (25). These phenotypes of the *Keap1*-null mice can be restored by simultaneous deletion of the *Nrf2* gene, indicating that the *Keap1*-null phenotype is attributable to the hyperactivation of Nrf2 (25).

When we deleted the *Nrf2* gene heterozygously in Keap1-deficient (i.e., *Keap1*$^{-/-}$::*Nrf2*$^{+/-}$) mice, we found a partial rescue of the severe phenotype of *Keap1*-null mice in the compound mutant mice. In contrast to the *Keap1*-null (*Keap1*$^{-/-}$::*Nrf2*$^{+/+}$) mice, the *Keap1*$^{-/-}$::*Nrf2*$^{+/-}$ mice survived to adulthood, as was the case for *Keap1*-null mice with the complete knockout of Nrf2 (*Keap1*$^{-/-}$::*Nrf2*$^{-/-}$). This indicates that deletion of a single allele

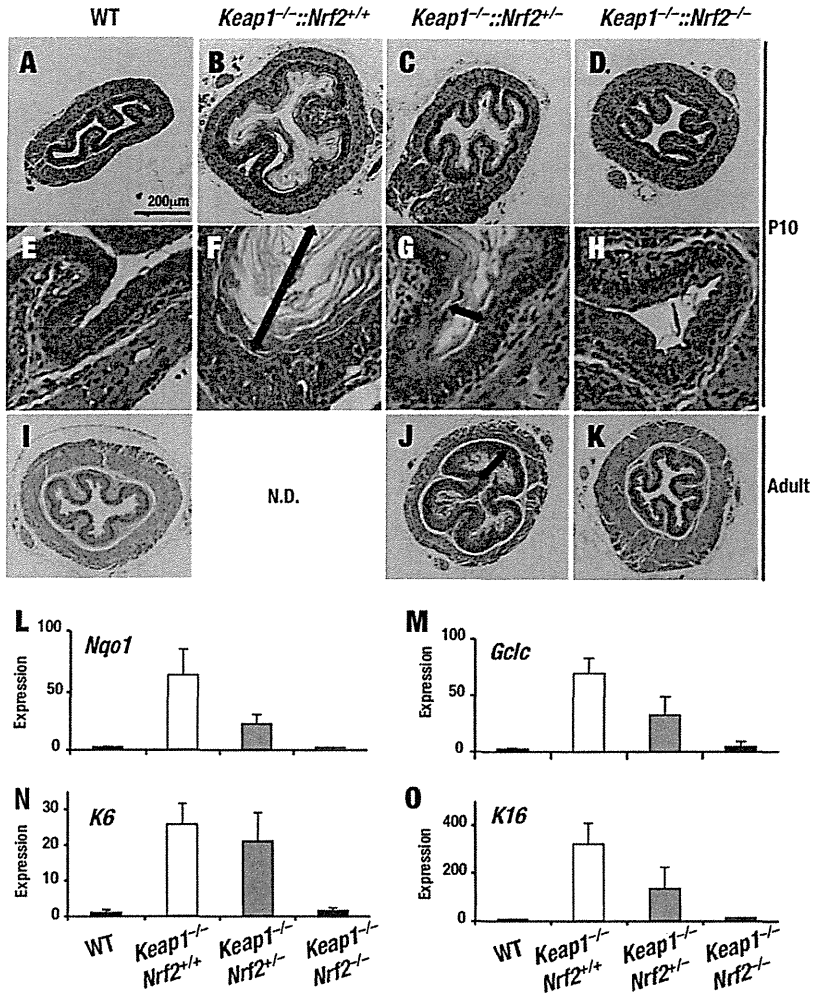

FIG 1 Heterozygous deletion of the *Nrf2* gene alleviates lethal phenotypes of Keap1-deficient mice. (A to K) H&E staining of transverse sections of the esophagus from P10 (A to H) and adult (I to K) mice. Lower (A to D) and higher (E to H) magnifications of the pictures are shown. Arrows indicate the thickened cornified layer. (L to O) Relative expression levels of the *Nqo1*, *Gclc*, *K6*, and *K16* genes compared with the level of 18S rRNA gene expression in the forestomachs of P10 mice. Data are the means ± SDs ($n = 3$). WT, wild type; N.D., no data.

of the *Nrf2* gene is sufficient to rescue the lethality caused by the Keap1 deficiency. We found that the average body weight of the *Keap1*$^{-/-}$::*Nrf2*$^{+/-}$ mice was less than that of the *Keap1*$^{-/-}$::*Nrf2*$^{-/-}$ mice in both males and females (see Fig. S1A and B in the supplemental material). Consistent with our previous observations (25), the *Keap1*$^{-/-}$::*Nrf2*$^{+/+}$ mice showed severe thickening of the cornified layers in the esophagus at 10 days after birth (Fig. 1B and F). On the contrary, the *Keap1*$^{-/-}$::*Nrf2*$^{+/-}$ mice showed clear improvement in the cornification and thickening (Fig. 1C and G). In adult *Keap1*$^{-/-}$::*Nrf2*$^{+/-}$ mouse esophagi, however, the thickening of the cornified layer became apparent (Fig. 1J). These results thus demonstrate that while the Nrf2 level synthesized from a single allele contributes to the esophageal phenotype to a certain extent in the *Keap1* knockout background (*Keap1*$^{-/-}$::*Nrf2*$^{+/-}$), it gives rise to a phenotype much milder than that resulting from the Nrf2 level synthesized from two alleles in the *Nrf2* wild-type background (*Keap1*$^{-/-}$::*Nrf2*$^{+/+}$).

Consistent with the esophageal phenotypes, the levels of expression of Nrf2 target genes, such as *Nqo1* [NAD(P)H:quinone oxidoreductase 1] and *Gclc* (glutamate-cysteine ligase catalytic subunit), and keratin-related genes, including *K6* (keratin 6) and *K16* (keratin 16), were lower in the forestomachs of *Keap1*$^{-/-}$::*Nrf2*$^{+/-}$ mice than in those of *Keap1*$^{-/-}$::*Nrf2*$^{+/+}$ mice but were higher than those in the forestomachs of *Keap1*$^{-/-}$::*Nrf2*$^{-/-}$ mice (Fig. 1L to O). Specifically, the levels of expression in the forestomachs of *Keap1*$^{-/-}$::*Nrf2*$^{+/-}$ mice were approximately half of the levels in *Keap1*$^{-/-}$::*Nrf2*$^{+/+}$ mice, indicating the presence of haploinsufficiency in *Nrf2* gene expression. These results thus indicate that the *Nrf2* gene dosage has an impact on Nrf2 activity *in vivo*.

Nrf2 synthesis is a critical determinant of cytoprotection capacity. Our next question was whether the Nrf2 transcription level affects the cellular capacity of cytoprotection even in the presence of Keap1-mediated Nrf2 degradation. To this end, we adopted thioglycolate-elicited mouse peritoneal macrophages as an experimental system, as this peritoneal macrophage system is well established as a system for testing the roles played by Nrf2 in the stress response (5). We first confirmed that in Nrf2 heterozygous

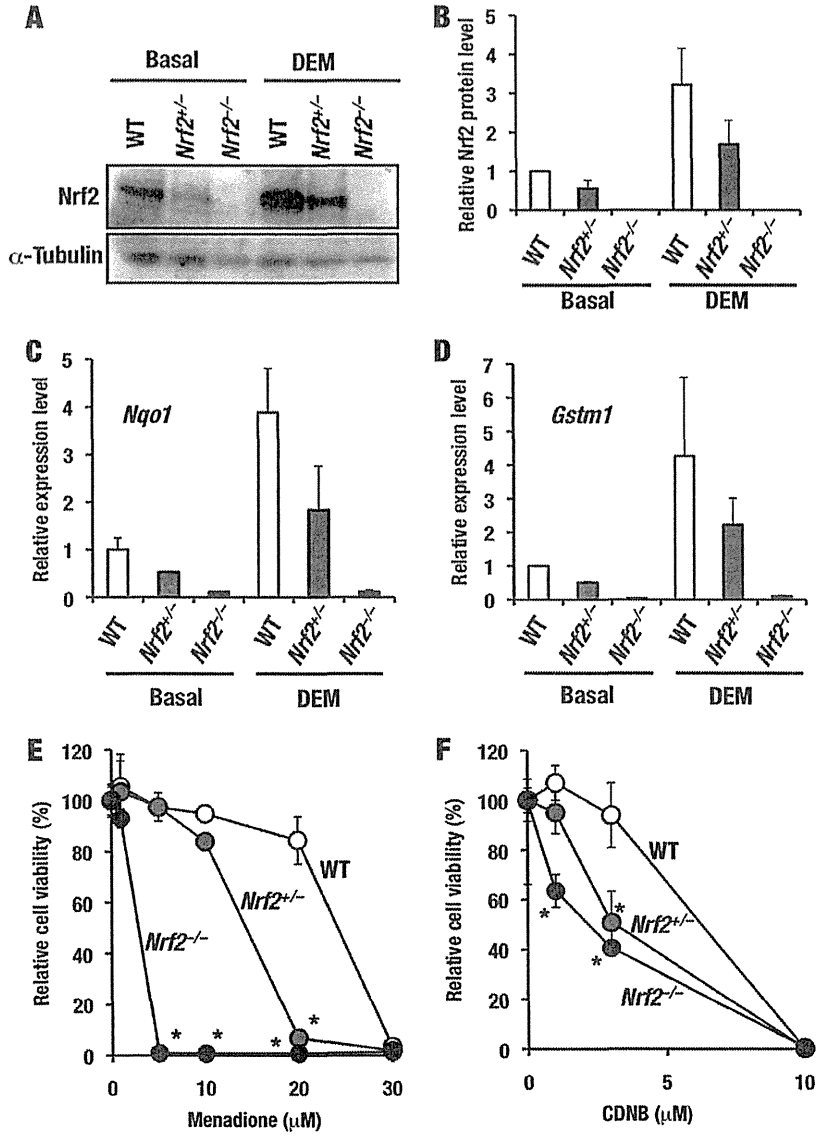

FIG 2 Heterozygous deletion of the *Nrf2* gene attenuates the ultimate activity of Nrf2 and impairs the oxidative stress response. (A) The Nrf2 protein level in macrophages from wild-type, $Nrf2^{+/-}$, and $Nrf2^{-/-}$ mice during the basal and DEM-induced states. (B) A graphical representation of the results in panel A is shown. Data are the means ± SDs ($n = 3$). (C and D) Relative *Nqo*1 (C) and *Gstm1* (D) expression levels compared with the level of 18S rRNA gene expression of macrophages from wild-type, $Nrf2^{+/-}$, and $Nrf2^{-/-}$ mice under basal and DEM-induced conditions. Data are the means ± SDs ($n = 3$). (E and F) Relative viability of macrophages from wild-type, $Nrf2^{+/-}$, and $Nrf2^{-/-}$ mice after 12 h of treatment with menadione (E) or CDNB (F). *, statistical significance compared with the result for wild-type cells ($P < 0.05$). Data are the means ± SDs ($n = 3$).

($Nrf2^{+/-}$) macrophages the *Nrf2* transcript level was almost half of that in wild-type cells (see Fig. S2A in the supplemental material), corresponding to the allele number difference in the *Nrf2* gene. Since Nrf2 is constitutively degraded in the basal state, we expected that in Nrf2 heterozygous cells the Nrf2 protein level would not change significantly from the wild-type level under normal conditions. To our surprise, however, the Nrf2 protein level in $Nrf2^{+/-}$ macrophages was clearly decreased compared with that in wild-type cells under basal conditions (Fig. 2A and B). When cells were stimulated with DEM, an electrophilic Nrf2 inducer, the Nrf2 protein level in $Nrf2^{+/-}$ cells became almost half of that in wild-type cells. Consistent with the Nrf2 protein level, the *Nqo1* and *Gstm1* (glutathione *S*-transferase, mu 1) mRNA level was significantly reduced under both basal and induced conditions (Fig. 2C and D). These results suggest that gene dosage does influence cellular Nrf2 activity and cytoprotection under both basal and induced conditions.

To test whether the decrease in the *Nrf2* allele reduces cytoprotective functions, we examined whether $Nrf2^{+/-}$ macrophages are more susceptible to the cytotoxic effect of xenobiotics than wild-type cells. We employed menadione, CDNB, and BITC, which are well-established stressors for testing the roles played by Nrf2 in the stress response (30). Consistent with the reduced expression of *Nqo1* and *Gstm1* in Nrf2 heterozy-

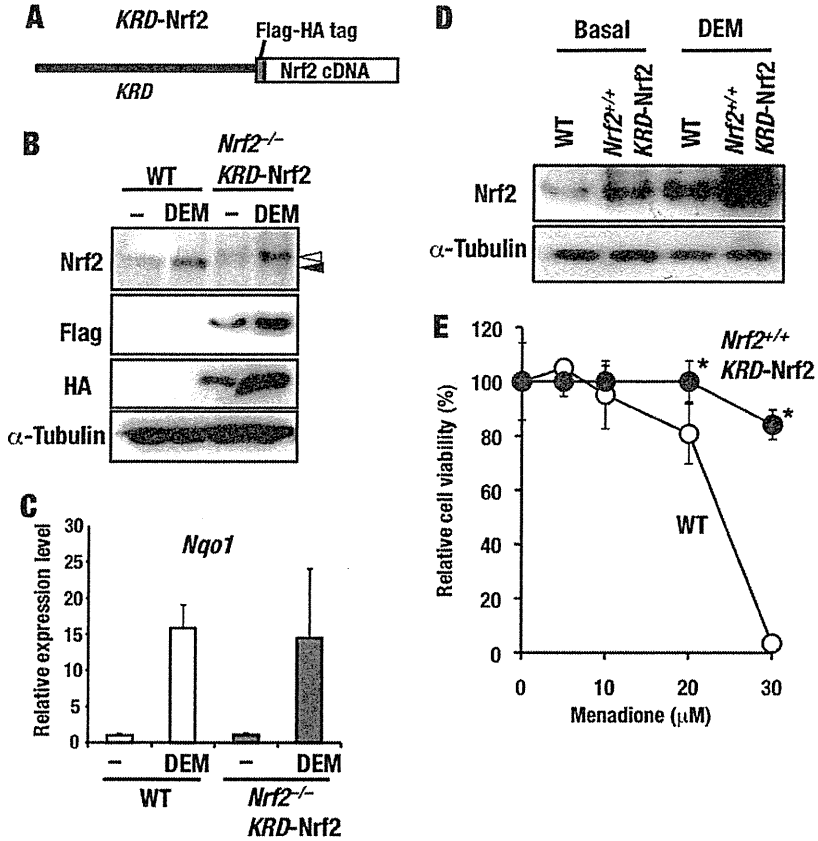

FIG 3 Increase in Nrf2 synthesis enhances Nrf2 activity and makes cells resistant to oxidative stress. (A) Structure of the transgene *KRD*-Nrf2. The Flag-HA double tag was fused to the N terminus of mouse Nrf2, and the fusion protein was expressed under the regulation of the Keap1 regulatory domain (*KRD*). (B) Level of transgene-derived Nrf2 expression in macrophages from $Nrf2^{-/-}$::*KRD*-Nrf2 mice. Closed and open arrowheads, endogenous Nrf2 and transgene-derived Flag-HA tagged Nrf2, respectively. (C) Relative levels of *Nqo1* expression compared with 18S rRNA gene expression in macrophages in the basal and DEM-induced states. Data are the means ± SDs ($n = 3$). (D) Nrf2 protein level in macrophages from wild-type and $Nrf2^{+/+}$::*KRD*-Nrf2 mice in the basal and DEM-induced states. Note the increase in the Nrf2 protein level in basal and DEM-treated $Nrf2^{+/+}$::*KRD*-Nrf2 macrophages. (E) Relative viability of macrophages from wild-type and $Nrf2^{+/+}$::*KRD*-Nrf2 mice after 12 h of treatment with menadione. Data are the means ± SDs ($n = 3$). *, statistical significance compared with the result for wild-type cells ($P < 0.05$).

gous macrophages, the cells appeared to be more susceptible to menadione, CDNB, and BITC than the wild-type cells but less susceptible to the insult than Nrf2-null macrophages (Fig. 2E and F; see Fig. S3 in the supplemental material), showing the haploinsufficiency of the *Nrf2* gene. These results thus demonstrate that the *Nrf2* mRNA expression level is critical for protecting cells from a wide range of xenobiotics.

Elevation of Nrf2 synthesis makes cells resistant to oxidative stress. *Keap1* gene knockout in mice results in an increase in Nrf2 protein levels. However, how the increase in *Nrf2* mRNA levels influences Nrf2 protein levels and cytoprotection is unclear. To assess the influence of *Nrf2* mRNA induction, we generated transgenic mouse lines that expressed Flag-HA-tagged Nrf2 under the control of the *Keap1* gene regulatory domain (*KRD*-Nrf2) (26) (Fig. 3A). Four independent lines were established for the *KRD*-Nrf2 transgene. We first examined whether transgene-derived Nrf2 protein was functional by crossing the transgenic mice with *Nrf2*-null mice ($Nrf2^{-/-}$::*KRD*-Nrf2). The transgenic mouse line expressed the transgene-derived Nrf2 protein at a level comparable to that of endogenous Nrf2 in macrophages under the basal and DEM-induced conditions (Fig. 3B), although the transgene-derived transcript was much more abundant than the endogenous Nrf2 transcript (see Fig. S2B in the supplemental material). This result is most likely due to the limited efficiency of translation from the transgene-derived mRNA, but the reasons for this are unknown. *Nqo1* expression was increased in the presence of DEM in $Nrf2^{-/-}$::*KRD*-Nrf2 macrophages to an extent similar to that in wild-type macrophages (Fig. 3C), indicating that the transgene-derived Nrf2 activated its target gene in response to DEM as efficiently as endogenous Nrf2.

We next analyzed the *KRD*-Nrf2 mice in the wild-type background ($Nrf2^{+/+}$::*KRD*-Nrf2). The Nrf2 protein level was robustly increased in the macrophages of $Nrf2^{+/+}$::*KRD*-Nrf2 mice compared with that in wild-type macrophages, irrespective of the induction status (Fig. 3D). When challenged with menadione, $Nrf2^{+/+}$::*KRD*-Nrf2 macrophages were more resistant to the cytotoxic effect of a high concentration of menadione than the wild-type control (Fig. 3E). Thus, although previous analyses argued that Nrf2 accumulated within the cells due to the derepression of rapid proteasome-dependent degradation, our present results demonstrate that the increase in *Nrf2* synthesis also effectively contributes to the increase in total cellular Nrf2 activity. Collectively, regulation of syn-

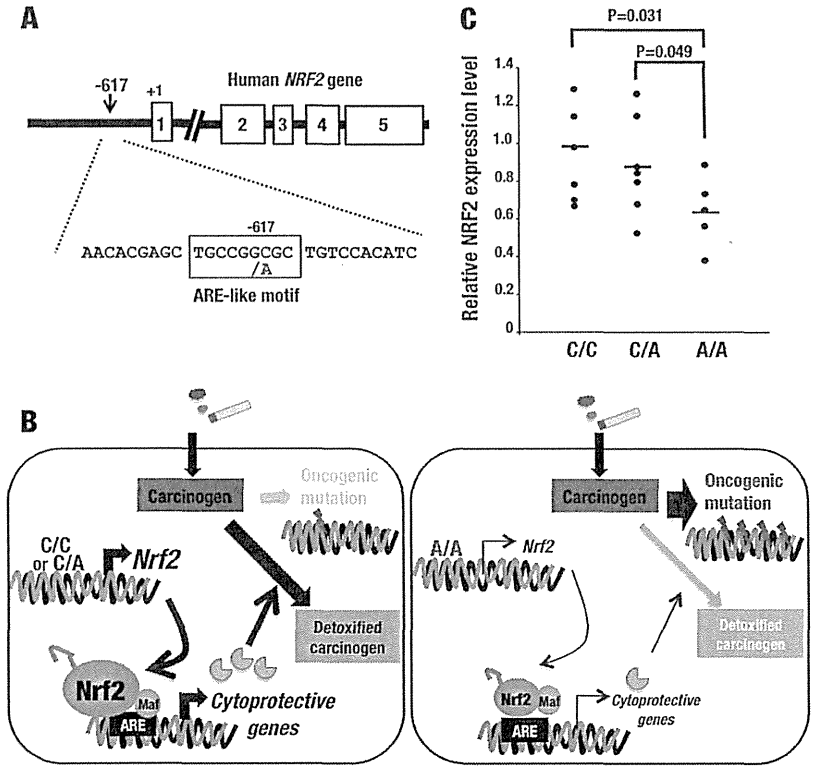

FIG 4 Genotypes of NRF2 rSNP-617 that affect *NRF2* gene expression. (A) Location of NRF2 rSNP-617 in the *NRF2* gene locus. The five exons are indicated by the numbered boxes. NRF2 rSNP-617 is located in the ARE-like motif in the promoter region of the *NRF2* gene. The polymorphic nucleotides are shown in red. (B) Schematic presentation of the putative mechanism for the association of NRF2 rSNP-617 and an increased risk of lung cancer. A/A homozygotes for NRF2 rSNP-617 significantly exhibit decreased expression of the *NRF2* gene and its downstream cytoprotective genes, resulting in the impaired detoxification of tobacco carcinogens and frequent oncogenic events. (C) Relative levels of human *NRF2* gene expression compared with *GAPDH* gene expression in immortalized lymphocytes of three different genotypes of NRF2 rSNP-617.

thesis and degradation in combination determines the cellular Nrf2 levels under basal and induced conditions.

Association of *NRF2* SNP and lung cancer susceptibility. Analyses of mouse models revealed that weakened transcription of the *Nrf2* gene results in the reduction of Nrf2 activity. We surmise that this reduction of NRF2 activity due to an *NRF2* SNP and reduced *NRF2* mRNA expression underlies various disease susceptibilities and/or pathophysiologies in humans. Therefore, we decided to examine the association of the *NRF2* SNP and lung cancer susceptibility.

A few SNPs within the *NRF2* gene have been described (20, 21). Of these SNPs, we focused on SNP rs6721961, located 617 bp upstream from the transcription start site of the gene (Fig. 4A), in this study. This SNP has been reported to be associated with the risk of acute lung injury (21), and its minor allele frequency varies among populations, as shown by the HapMap and 1,000 Genomes Projects (http://www.ncbi.nlm.nih.gov/projects/SNP/snp_ref.cgi?rs=6721961). We refer to rSNP rs6721961 as NRF2 rSNP-617 in this study. We conducted a case-control study consisting of 2,701 lung cancer patients (1,987 patients with ADC, 411 patients with squamous cell carcinoma [SQC], and 303 patients with small-cell lung carcinoma [SCC]) and 1,167 controls who had distributions of age, gender, ethnicity, and smoking status similar to those of the patient population (Table 1). All 3,868 case and control subjects were genotyped for the NRF2 rSNP-617, and the association of the genotypes with the risk for development of lung cancers was examined (Table 2). Notably, the frequency of the minor allele (i.e., the A allele, which causes a low level of expression, as described below) for this SNP was more prevalent in lung cancer patients than in controls (Table 2). Homozygotes for the minor allele (A/A) and the recessive mode (A/A homozygotes versus C/A heterozygotes plus C/C homozygotes) for the minor allele showed significant associations with overall lung cancer risk (odds ratio [OR] = 1.54 [$P = 0.0084$] and OR = 1.53 [$P = 0.0083$], respectively).

We next examined the association of NRF2 rSNP-617 with lung cancer risk according to clinicopathological factors. Minor homozygotes showed similarly increased risks for all histological types of lung cancers, including ADC, SQC, and SCC (Table 2). The homozygotes showed a higher risk in ever smokers than in never smokers (OR = 2.57 [$P = 0.00041$] versus OR = 1.13 [$P = 0.58$]) (Table 2).

We further examined the association of NRF2 rSNP-617 with the risk for developing lung ADC according to oncogenic pathway, i.e., *EGFR* and *KRAS* driver gene mutations (31) (Table 3). Minor homozygotes showed similarly increased risks for both lung ADC-bearing *EGFR* and *KRAS* mutations, with the association of ADC with the *EGFR* mutation being significant due to a large number of subjects (OR = 1.55 [$P = 0.0497$] and OR = 1.39 [$P = 0.47$], respectively). In contrast, an increase in the OR was

TABLE 1 Profiles of lung cancer cases and control cases that were analyzed in this study

Variable	Controls	Cases[a]						
			ADC					
				Mutation status				
		All	All	*EGFR*	*KRAS*	None	SQC	SCC
Total no. of cases	1,167	2,701	1,987	600	114	489	411	303
Mean ± SD age (yr)	49 ± 11	59 ± 11	58 ± 11	59 ± 10	59 ± 8	58 ± 10	61 ± 8	62 ± 11
No. (%) of subjects of the following sex:								
Male	725 (62)	1,746 (65)	1,137 (57)	243 (41)	81 (71)	315 (64)	366 (89)	243 (80)
Female	442 (38)	955 (35)	850 (43)	357 (59)	33 (29)	174 (36)	45 (11)	60 (20)
No. (%) of subjects with the following smoking status:								
Never smoker	760 (65)	884 (33)	853 (43)	361 (60)	30 (26)	192 (39)	17 (4)	14 (5)
Ever smoker	407 (35)	1,817 (67)	1,134 (57)	239 (40)	84 (74)	297 (61)	394 (96)	289 (95)

[a] ADC, adenocarcinoma; SQC, squamous cell carcinoma; SCC, small-cell carcinoma.

not evident for lung ADC without *EGFR* and *KRAS* mutations (OR = 1.14, $P = 0.61$). These results therefore indicate that minor homozygotes (A/A) of the NRF2 rSNP-617 are associated with the risk for lung cancers, especially ever smokers (Fig. 4B). Notably, in lung ADC cases, the association was evident in cancers harboring *EGFR* mutations.

NRF2 rSNP-617 affects gene expression in lymphocytes. The NRF2 rSNP-617 coincides with the ARE motif, which is important

TABLE 2 Genotype distribution for the rs6721961 SNP between controls and cancer cases

Category[a]	Genotype	No. (%) of subjects		Adjusted OR (95% CI)	*P*
		Controls	Cancer cases		
All	C/C	627 (53.7)	1,466 (54.3)	Reference	
	C/A	477 (40.9)	1,026 (38.0)	1.02 (0.87–1.19)	0.85[b]
	A/A	63 (5.4)	209 (7.7)	1.54 (1.12–2.16)	0.0084[b]
	Dominant			1.08 (0.92–1.26)	0.34[b]
	Recessive			1.53 (1.11–2.12)	0.0083[b]
ADC	C/C		1,071 (53.9)	Reference	
	C/A		761 (38.3)	1.02 (0.87–1.21)	0.77[b]
	A/A		155 (7.8)	1.55 (1.12–2.18)	0.0088[b]
	Dominant			1.09 (0.93–1.27)	0.30[b]
	Recessive			1.53 (1.11–2.13)	0.0092[b]
SQC	C/C		230 (56.0)	Reference	
	C/A		149 (36.3)	0.89 (0.66–1.21)	0.46[b]
	A/A		32 (7.8)	2.05 (1.11–3.85)	0.023[b]
	Dominant			1.00 (0.75–1.33)	0.99[b]
	Recessive			2.19 (1.18–4.12)	0.013[b]
SCC	C/C		165 (54.5)	Reference	
	C/A		116 (38.3)	1.00 (0.72–1.39)	0.99[b]
	A/A		22 (7.3)	1.82 (0.91–3.68)	0.092[b]
	Dominant			1.08 (0.79–1.48)	0.63[b]
	Recessive			1.83 (0.93–3.61)	0.082[b]
Never smoker	C/C	408 (53.7)	476 (53.8)	Reference	
	C/A	302 (40.0)	344 (39.0)	1.12 (0.89–1.41)	0.33[c]
	A/A	50 (6.6)	64 (7.2)	1.19 (0.77–1.83)	0.44[c]
	Dominant			1.13 (0.91–1.41)	0.26[c]
	Recessive			1.13 (0.74–1.73)	0.58[c]
Ever smoker	C/C	219 (53.8)	990 (54.5)	Reference	
	C/A	175 (43.0)	682 (37.5)	0.94 (0.75–1.18)	0.58[c]
	A/A	13 (3.2)	145 (8.0)	2.48 (1.42–4.70)	8.9×10^{-4}[c]
	Dominant			1.05 (0.84–1.31)	0.68[c]
	Recessive			2.57 (1.49–4.86)	4.1×10^{-4}[c]

[a] ADC, adenocarcinoma; SQC, squamous cell carcinoma; SCC, small-cell carcinoma.
[b] Adjusted for sex, age, and smoking status.
[c] Adjusted for sex and age.

TABLE 3 Association of the rs6721961 SNP and risk for development of lung ADC with or without the *EGFR* or *KRAS* mutation

Category	Genotype	No. (%) of subjects		Adjusted OR[a] (95% CI)	*P*
		Controls	Cancer cases		
EGFR mutation	C/C	627 (53.7)	327 (54.5)	Reference	
	C/A	477 (40.9)	224 (37.3)	1.00 (0.80–1.25)	1.00
	A/A	63 (5.4)	49 (8.2)	1.55 (1.00–2.38)	0.0497
	Dominant			1.07 (0.86–1.32)	0.56
	Recessive			1.55 (1.01–2.36)	0.044
KRAS mutation	C/C		63 (55.3)	Reference	
	C/A		44 (38.6)	0.95 (0.62–1.44)	0.80
	A/A		7 (6.1)	1.39 (0.54–3.10)	0.47
	Dominant			0.99 (0.66–1.48)	0.97
	Recessive			1.55 (0.61–3.44)	0.33
None	C/C		273 (55.8)	Reference	
	C/A		190 (38.9)	0.99 (0.78–1.25)	0.95
	A/A		26 (5.3)	1.14 (0.68–1.90)	0.61
	Dominant			1.00 (0.80–1.26)	0.95
	Recessive			1.14 (0.68–1.87)	0.61

[a] Adjusted for sex, age, and smoking status.

for *NRF2* expression in a feed-forward activation mechanism. Because the A allele-containing ARE is mutated, the transcription level of the *NRF2* gene is expected to be lower in the A allele case than in the C allele case, but no conclusive answer to whether the NRF2 rSNP-617 affects transcription of the *NRF2* gene *in vivo* has been obtained. To address this issue, we quantified the *NRF2* mRNA in immortalized human lymphocytes with distinct NRF2 rSNP-617 genotypes (Fig. 4C). We found that the *NRF2* mRNA levels were significantly lower in A/A homozygotes than in C/A heterozygotes and C/C homozygotes by approximately 40% ($P = 0.031$ and 0.049, respectively). No significant difference was observed between C/C homozygotes and C/A heterozygotes ($P = 0.47$), indicating that a homozygous nucleotide change from C to A at NRF2 rSNP-617 significantly decreased *NRF2* mRNA expression. Consistent with the NRF2 mRNA level, the levels of expression of *tert*-butylhydroquinone-induced NRF2 protein (see Fig. S4 in the supplemental material) and *NQO1* mRNA (see Fig. S5 in the supplemental material) were lower in A/A homozygote than in C/C genotype lymphocytes. These results strongly support the notion that the level of *NRF2* gene transcription is important for the role of NRF2 in cytoprotection, including cancer prevention (Fig. 4B).

DISCUSSION

In this study, we showed clinical and experimental lines of evidence that the final Nrf2 protein level in cells is under dual regulation at the protein degradation level and gene transcription level. The characteristic phenotypes of *Keap1*-null mice, i.e., hyperkeratosis and growth retardation, which are attributable to high Nrf2 activity, are significantly improved by deletion of a single allele of the *Nrf2* gene. Under physiological conditions (in the presence of Keap1-dependent Nrf2 degradation), a decrease in the *Nrf2* mRNA level markedly attenuates the final Nrf2 protein level, which in turn increases the susceptibility of mice to a wide range of xenobiotics. Conversely, when the Nrf2 mRNA level is increased, the Nrf2 protein level is enhanced and the cellular defense against oxidative stress is augmented. In excellent agreement with these results, we found that minor A/A homozygotes of NRF2 rSNP-617 exhibit significantly decreased *NRF2* gene expression and, consequently, increased the risk of lung cancers, especially in ever smokers. Thus, as summarized in Fig. 5, coordinated synthesis and degradation of Nrf2 are critically important for the maintenance of cellular redox homeostasis. Of note, we verified in this study that the transcription level of the *NRF2* gene is indeed important for the roles that NRF2 plays in cytoprotection.

The experiments utilizing genetically engineered mice demonstrate that a decrease in the *Nrf2* transcript to approximately half of its level is physiologically critical. This observation supports the contention that minor A/A homozygotes of NRF2 rSNP-617 are susceptible to lung cancers because of the 40% reduction in the *NRF2* transcript. Notably, changes in *Nrf2* transcript level alter the Nrf2 protein level, even in the basal state, in which Keap1 actively degrades Nrf2. This observation has led us to consider the kinetic properties of Keap1-dependent degradation of Nrf2. We surmise two possible models here. One is the threshold model, in which the Keap1-based ubiquitin E3 ligase system degrades Nrf2 efficiently and completely if its abundance is below a certain threshold. The other is the probability model, in which the Keap1-based ubiquitin ligase system degrades a certain ratio of Nrf2 irrespective of its abundance. Our present results support the latter model, as the status of Nrf2 synthesis exquisitely reflects the Nrf2 protein level, especially under basal conditions.

The analysis of lung cancer patient cohort and non-cancer patient populations revealed that NRF2 rSNP-617 has an association with susceptibility to lung cancer, especially for ever smokers. Although smoking is the top-ranked risk factor for lung cancer, little is known about genetic variations that increase the cancer risk related to smoking. Previous large-scale genome-wide association studies revealed the associations between variations in the nicotine receptor gene (32, 33) or the CYP1A1 and CYP2A6 detoxification enzyme genes (34) and susceptibility in smoking-associated lung cancers. Because oxidative stress has been well established to be one of the main factors in smoking-associated carcinogenesis, the result of our clinical study is in very good agreement with the function of Nrf2 as a key regulator of the cellular response against oxidative stresses.

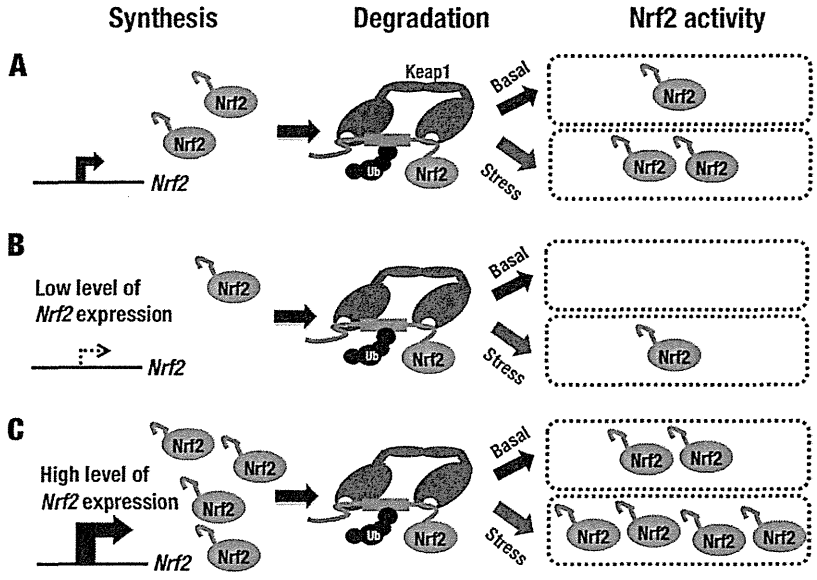

FIG 5 Dual regulation of Nrf2 activity by synthesis and degradation. (A) When an adequate level of the *Nrf2* transcript is supplied, the Nrf2 protein is maintained at low levels by Keap1-mediated degradation under the basal condition, and a relatively high level of the Nrf2 protein is accumulated after the inactivation of Keap1. (B) When the *Nrf2* transcription level is low, the Nrf2 protein is decreased in both the basal and induced states. (C) When a high *Nrf2* transcript level is achieved, a large amount of Nrf2 is produced in both the basal and induced states.

In addition to NRF2 rSNP-617, there appear to be other causes that result in a reduction of Nrf2 synthesis. Indeed, *Nrf2* expression is decreased in aged smokers and patients with chronic obstructive pulmonary diseases (35). We showed that transgenic overexpression of Nrf2 significantly increases the Nrf2 protein level and makes cells resistant to oxidative stress. These observations suggest that induction of the Nrf2 transcript is an effective approach for enhancing the activity of Nrf2. To date, several factors have been found to increase the Nrf2 transcript level, including Nrf2 itself by autoactivation (19), the aryl hydrocarbon receptor (36), and Jun (37).

Increasing numbers of studies have revealed that NRF2 is also involved in the malignant progression of various human cancers (13–15). Constitutive activation of NRF2 gives a strong advantage to cancer cells by conferring chemo- and radioresistance and accelerating proliferation (38–40). A recent study demonstrated that NRF2 is constitutively activated in lung cancer cells bearing *EGFR* mutations (41). Transcriptional activation of *NRF2* by the RAS oncogenic pathway also substantially contributes to the enhancement of NRF2 activity in cancer (42). Accordingly, we expect that *EGFR* and *KRAS* mutations are associated with NRF2 rSNP-617. We found that there are associations of the minor A/A homozygotes with the risk for developing lung cancers with *EGFR* and *KRAS* mutations (Table 3). One plausible explanation for this association is that *EGFR* and *KRAS* mutations may compensate for the compromised transcription of *NRF2*, allowing the A/A homozygous cancer cells to achieve a sufficiently high level of NRF2 activity.

In summary, Nrf2 has been considered a transcription factor which is mainly regulated by a posttranslational derepression mechanism. In this study, we found that weakened transcription of the *Nrf2* gene provides a basis for the development of lung cancers, possibly through the reduced expression of cytoprotective enzymes. This observation leads to the notion that in addition to control over proteasomal degradation and derepression from degradation/repression, transcriptional regulation of the *Nrf2* gene in response to various signals/insults is an important pathway in determining cellular Nrf2 levels. Collectively, the contribution of NRF2 to these physiological and pathological processes is regulated at various nodes, and the delineation of these mechanisms is a critical step toward a better understanding of our defense machinery.

ACKNOWLEDGMENTS

We thank Eriko Naganuma, Hiromi Suda, Yukie Kawatani, Naoko Okada, and Akiko Kokubu for technical assistance. We also thank Liam Baird for discussion and advice.

This work was supported in part by Grants-in-Aid for Creative Scientific Research and Scientific Research from JSPS, the Target Protein Program from MEXT, the Tohoku University Global COE Program for Conquest of Signal Transduction Diseases with Network Medicine, CREST from JST, the NAITO Foundation, the Takeda Foundation, and grants-in-aid from the Ministry of Health, Labor, and Welfare for the 3rd-Term Comprehensive 10-Year Strategy for Cancer Control and Research on Applying Health Technology.

REFERENCES

1. Motohashi H, Yamamoto M. 2004. Nrf2-Keap1 defines a physiologically important stress response mechanism. Trends Mol. Med. 10:549–557.
2. Friling RS, Bensimon A, Tichauer Y, Daniel V. 1990. Xenobiotic-inducible expression of murine glutathione S-transferase Ya subunit gene is controlled by an electrophile-responsive element. Proc. Natl. Acad. Sci. U. S. A. 87:6258–6262.
3. Rushmore TH, Morton MR, Pickett CB. 1991. The antioxidant responsive element. Activation by oxidative stress and identification of the DNA consensus sequence required for functional activity. J. Biol. Chem. 266:11632–11639.
4. Kobayashi M, Yamamoto M. 2006. Nrf2-Keap1 regulation of cellular defense mechanisms against electrophiles and reactive oxygen species. Adv. Enzyme Regul. 46:113–140.
5. Ishii T, Itoh K, Takahashi S, Sato H, Yanagawa T, Katoh Y, Bannai S,

Yamamoto M. 2000. Transcription factor Nrf2 coordinately regulates a group of oxidative stress-inducible genes in macrophages. J. Biol. Chem. 275:16023–16029.
6. Itoh K, Chiba T, Takahashi S, Ishii T, Igarashi K, Katoh Y, Oyake T, Hayashi N, Satoh K, Hatayama I, Yamamoto M, Nabeshima Y. 1997. An Nrf2/small Maf heterodimer mediates the induction of phase II detoxifying enzyme genes through antioxidant response elements. Biochem. Biophys. Res. Commun. 236:313–322.
7. Aoki Y, Sato H, Nishimura N, Takahashi S, Itoh K, Yamamoto M. 2001. Accelerated DNA adduct formation in the lung of the Nrf2 knockout mouse exposed to diesel exhaust. Toxicol. Appl. Pharmacol. 173:154–160.
8. Cho HY, Jedlicka AE, Reddy SP, Kensler TW, Yamamoto M, Zhang LY, Kleeberger SR. 2002. Role of NRF2 in protection against hyperoxic lung injury in mice. Am. J. Respir. Cell Mol. Biol. 26:175–182.
9. Enomoto A, Itoh K, Nagayoshi E, Haruta J, Kimura T, O'Connor T, Harada T, Yamamoto M. 2001. High sensitivity of Nrf2 knockout mice to acetaminophen hepatotoxicity associated with decreased expression of ARE-regulated drug metabolizing enzymes and antioxidant genes. Toxicol. Sci. 59:169–177.
10. Iida K, Itoh K, Kumagai Y, Oyasu R, Hattori K, Kawai K, Shimazui T, Akaza H, Yamamoto M. 2004. Nrf2 is essential for the chemopreventive efficacy of oltipraz against urinary bladder carcinogenesis. Cancer Res. 64:6424–6431.
11. Ramos-Gomez M, Kwak MK, Dolan PM, Itoh K, Yamamoto M, Talalay P, Kensler TW. 2001. Sensitivity to carcinogenesis is increased and chemoprotective efficacy of enzyme inducers is lost in nrf2 transcription factor-deficient mice. Proc. Natl. Acad. Sci. U. S. A. 98:3410–3415.
12. Xu C, Huang MT, Shen G, Yuan X, Lin W, Khor TO, Conney AH, Kong AN. 2006. Inhibition of 7,12-dimethylbenz(a)anthracene-induced skin tumorigenesis in C57BL/6 mice by sulforaphane is mediated by nuclear factor E2-related factor 2. Cancer Res. 66:8293–8296.
13. Padmanabhan B, Tong KI, Ohta T, Nakamura Y, Scharlock M, Ohtsuji M, Kang MI, Kobayashi A, Yokoyama S, Yamamoto M. 2006. Structural basis for defects of Keap1 activity provoked by its point mutations in lung cancer. Mol. Cell 21:689–700.
14. Shibata T, Ohta T, Tong KI, Kokubu A, Odogawa R, Tsuta K, Asamura H, Yamamoto M, Hirohashi S. 2008. Cancer related mutations in NRF2 impair its recognition by Keap1-Cul3 E3 ligase and promote malignancy. Proc. Natl. Acad. Sci. U. S. A. 105:13568–13573.
15. Singh A, Misra V, Thimmulappa RK, Lee H, Ames S, Hoque MO, Herman JG, Baylin SB, Sidransky D, Gabrielson E, Brock MV, Biswal S. 2006. Dysfunctional KEAP1-NRF2 interaction in non-small-cell lung cancer. PLoS Med. 3:e420. doi:10.1371/journal.pmed.0030420.
16. Itoh K, Wakabayashi N, Katoh Y, Ishii T, Igarashi K, Engel JD, Yamamoto M. 1999. Keap1 represses nuclear activation of antioxidant responsive elements by Nrf2 through binding to the amino-terminal Neh2 domain. Genes Dev. 13:76–86.
17. Kobayashi A, Kang MI, Watai Y, Tong KI, Shibata T, Uchida K, Yamamoto M. 2006. Oxidative and electrophilic stresses activate Nrf2 through inhibition of ubiquitination activity of Keap1. Mol. Cell. Biol. 26:221–229.
18. Itoh K, Wakabayashi N, Katoh Y, Ishii T, O'Connor T, Yamamoto M. 2003. Keap1 regulates both cytoplasmic-nuclear shuttling and degradation of Nrf2 in response to electrophiles. Genes Cells 8:379–391.
19. Kwak MK, Itoh K, Yamamoto M, Kensler TW. 2002. Enhanced expression of the transcription factor Nrf2 by cancer chemopreventive agents: role of antioxidant response element-like sequences in the nrf2 promoter. Mol. Cell. Biol. 22:2883–2892.
20. Yamamoto T, Yoh K, Kobayashi A, Ishii Y, Kure S, Koyama A, Sakamoto T, Sekizawa K, Motohashi H, Yamamoto M. 2004. Identification of polymorphisms in the promoter region of the human NRF2 gene. Biochem. Biophys. Res. Commun. 321:72–79.
21. Marzec JM, Christie JD, Reddy SP, Jedlicka AE, Vuong H, Lanken PN, Aplenc R, Yamamoto T, Yamamoto M, Cho HY, Kleeberger SR. 2007. Functional polymorphisms in the transcription factor NRF2 in humans increase the risk of acute lung injury. FASEB J. 21:2237–2246.
22. Bouligand J, Cabaret O, Canonico M, Verstuyft C, Dubert L, Becquemont L, Guiochon-Mantel A, Scarabin PY, Estrogen and Thromboembolism Risk (ESTHER) Study Group. 2011. Effect of NFE2L2 genetic polymorphism on the association between oral estrogen therapy and the risk of venous thromboembolism in postmenopausal women. Clin. Pharmacol. Ther. 89:60–64.
23. Masuko H, Sakamoto T, Kaneko Y, Iijima H, Naito T, Noguchi E, Hirota T, Tamari M, Hizawa N. 2011. An interaction between Nrf2 polymorphisms and smoking status affects annual decline in FEV1: a longitudinal retrospective cohort study. BMC Med. Genet. 12:97. doi:10.1186/1471-2350-12-97.
24. Marczak ED, Marzec J, Zeldin DC, Kleeberger SR, Brown NJ, Pretorius M, Lee CR. 2012. Polymorphisms in the transcription factor NRF2 and forearm vasodilator responses in humans. Pharmacogenet. Genomics 22:620–628.
25. Wakabayashi N, Itoh K, Wakabayashi J, Motohashi H, Noda S, Takahashi S, Imakado S, Kotsuji T, Otsuka F, Roop DR, Harada T, Engel JD, Yamamoto M. 2003. Keap1-null mutation leads to postnatal lethality due to constitutive Nrf2 activation. Nat. Genet. 35:238–245.
26. Yamamoto T, Suzuki T, Kobayashi A, Wakabayashi J, Maher J, Motohashi H, Yamamoto M. 2008. Physiological significance of reactive cysteine residues of Keap1 in determining Nrf2 activity. Mol. Cell. Biol. 28:2758–2770.
27. Maruyama A, Tsukamoto S, Nishikawa K, Yoshida A, Harada N, Motojima K, Ishii T, Nakane A, Yamamoto M, Itoh K. 2008. Nrf2 regulates the alternative first exons of CD36 in macrophages through specific antioxidant response elements. Arch. Biochem. Biophys. 477:139–145.
28. Travis WD. 2004. Pathology and genetics: tumours of the lung, pleura, thymus and heart. International Agency for Research on Cancer Press, Lyon, France.
29. Takano T, Ohe Y, Sakamoto H, Tsuta K, Matsuno Y, Tateishi U, Yamamoto S, Nokihara H, Yamamoto N, Sekine I, Kunitoh H, Shibata T, Sakiyama T, Yoshida T, Tamura T. 2005. Epidermal growth factor receptor gene mutations and increased copy numbers predict gefitinib sensitivity in patients with recurrent non-small-cell lung cancer. J. Clin. Oncol. 23:6829–6837.
30. Higgins LG, Kelleher MO, Eggleston IM, Itoh K, Yamamoto M, Hayes JD. 2009. Transcription factor Nrf2 mediates an adaptive response to sulforaphane that protects fibroblasts in vitro against the cytotoxic effects of electrophiles, peroxides and redox-cycling agents. Toxicol. Appl. Pharmacol. 237:267–280.
31. Kosaka T, Yatabe Y, Endoh H, Kuwano H, Takahashi T, Mitsudomi T. 2004. Mutations of the epidermal growth factor receptor gene in lung cancer: biological and clinical implications. Cancer Res. 64:8919–8923.
32. McKay JD, Hung RJ, Gaborieau V, Boffetta P, Chabrier A, Byrnes G, Zaridze D, Mukeria A, Szeszenia-Dabrowska N, Lissowska J, Rudnai P, Fabianova E, Mates D, Bencko V, Foretova L, Janout V, McLaughlin J, Shepherd F, Montpetit A, Narod S, Krokan HE, Skorpen F, Elvestad MB, Vatten L, Njølstad I, Axelsson T, Chen C, Goodman G, Barnett M, Loomis MM, Lubiński J, Matyjasik J, Lener M, Oszutowska D, Field J, Liloglou T, Xinarianos G, Cassidy A, Vineis P, Clavel-Chapelon F, Palli D, Tumino R, Krogh V, Panico S, González CA, Ramón Quirós J, Martínez C, Navarro C, Ardanaz E, Larrañaga N, et al. 2008. Lung cancer susceptibility locus at 5p15.33. Nat. Genet. 40:1404–1406.
33. Wang Y, Broderick P, Webb E, Wu X, Vijayakrishnan J, Matakidou A, Qureshi M, Dong Q, Gu X, Chen WV, Spitz MR, Eisen T, Amos CI, Houlston RS. 2008. Common 5p15.33 and 6p21.33 variants influence lung cancer risk. Nat. Genet. 40:1407–1409.
34. Rotunno M, Yu K, Lubin JH, Consonni D, Pesatori AC, Goldstein AM, Goldin LR, Wacholder S, Welch R, Burdette L, Chanock SJ, Bertazzi PA, Tucker MA, Caporaso NE, Chatterjee N, Bergen AW, Landi MT. 2009. Phase I metabolic genes and risk of lung cancer: multiple polymorphisms and mRNA expression. PLoS One 4:e5652. doi:10.1371/journal.pone.0005652.
35. Suzuki M, Betsuyaku T, Ito Y, Nagai K, Nasuhara Y, Kaga K, Kondo S, Nishimura M. 2008. Down-regulated NF-E2-related factor 2 in pulmonary macrophages of aged smokers and patients with chronic obstructive pulmonary disease. Am. J. Respir. Cell Mol. Biol. 39:673–682.
36. Miao W, Hu L, Scrivens PJ, Batist G. 2005. Transcriptional regulation of NF-E2 p45-related factor (NRF2) expression by the aryl hydrocarbon receptor-xenobiotic response element signaling pathway: direct cross-talk between phase I and II drug-metabolizing enzymes. J. Biol. Chem. 280:20340–20348.
37. Meixner A, Karreth F, Kenner L, Penninger JM, Wagner EF. 2010. Jun and JunD-dependent functions in cell proliferation and stress response. Cell Death Differ. 17:1409–1419.
38. Mitsuishi Y, Taguchi K, Kawatani Y, Shibata T, Nukiwa T, Aburatani

H, Yamamoto M, Motohashi H. 2012. Nrf2 redirects glucose and glutamine into anabolic pathways in metabolic reprogramming. Cancer Cell 22:66–79.
39. Shibata T, Kokubu A, Saito S, Narisawa-Saito M, Sasaki H, Aoyagi K, Yoshimatsu Y, Tachimori Y, Kushima R, Kiyono T, Yamamoto M. 2011. NRF2 mutation confers malignant potential and resistance to chemoradiation therapy in advanced esophageal squamous cancer. Neoplasia 13:864–873.
40. Singh A, Boldin-Adamsky S, Thimmulappa RK, Rath SK, Ashush H, Coulter J, Blackford A, Goodman SN, Bunz F, Watson WH, Gabrielson E, Feinstein E, Biswal S. 2008. RNAi-mediated silencing of nuclear factor erythroid-2-related factor 2 gene expression in non-small cell lung cancer inhibits tumor growth and increases efficacy of chemotherapy. Cancer Res. 68: 7975–7984.
41. Yamadori T, Ishii Y, Homma S, Morishima Y, Kurishima K, Itoh K, Yamamoto M, Minami Y, Noguchi M, Hizawa N. 2012. Molecular mechanisms for the regulation of Nrf2-mediated cell proliferation in non-small-cell lung cancers. Oncogene 31:4768–4777.
42. DeNicola GM, Karreth FA, Humpton TJ, Gopinathan A, Wei C, Frese K, Mangal D, Yu KH, Yeo CJ, Calhoun ES, Scrimieri F, Winter JM, Hruban RH, Iacobuzio-Donahue C, Kern SE, Blair IA, Tuveson DA. 2011. Oncogene-induced Nrf2 transcription promotes ROS detoxification and tumorigenesis. Nature 475:106–109.
43. Hayes JD, McMahon M, Chowdhry S, Dinkova-Kostova AT. 2010. Cancer chemoprevention mechanisms mediated through the Keap1-Nrf2 pathway. Antioxid. Redox Signal. 13:1713–1748.
44. Kobayashi A, Kang MI, Okawa H, Ohtsuji M, Zenke Y, Chiba T, Igarashi K, Yamamoto M. 2004. Oxidative stress sensor Keap1 functions as an adaptor for Cul3-based E3 ligase to regulate proteasomal degradation of Nrf2. Mol. Cell. Biol. 24:7130–7139.

Cancer Science
The official journal of the Japanese Cancer Association JCA

Identification of a lung adenocarcinoma cell line with CCDC6-RET fusion gene and the effect of RET inhibitors *in vitro* and *in vivo*

Makito Suzuki,[1,2,11] Hideki Makinoshima,[1,11] Shingo Matsumoto,[1,3] Ayako Suzuki,[4] Sachiyo Mimaki,[1] Koutatsu Matsushima,[1,2] Kiyotaka Yoh,[3] Koichi Goto,[3] Yutaka Suzuki,[4] Genichiro Ishii,[5] Atsushi Ochiai,[5] Koji Tsuta,[6] Tatsuhiro Shibata,[7] Takashi Kohno,[8] Hiroyasu Esumi[9] and Katsuya Tsuchihara[1,2,10]

[1]Division of Translational Research, Research Center for Innovative Oncology, National Cancer Center Hospital East, Kashiwa, Chiba; [2]Department of Integrated Biosciences, Graduate School of Frontier Sciences, The University of Tokyo, Kashiwa, Chiba; [3]Division of Thoracic Oncology, National Cancer Center Hospital East, Kashiwa, Chiba; [4]Department of Medical Genome Sciences, Graduate School of Frontier Sciences, The University of Tokyo, Kashiwa, Chiba; [5]Division of Pathology, Research Center for Innovative Oncology, National Cancer Center Hospital East, Kashiwa, Chiba; [6]Division of Pathology and Clinical Laboratories, National Cancer Center Hospital, Tokyo; Divisions of [7]Cancer Genomics; [8]Genome Biology, National Cancer Center Research Institute, Tokyo; [9]National Cancer Center Hospital East, Kashiwa, Chiba, Japan

(Received December 4, 2012/Revised April 1, 2013/Accepted April 1, 2013/Accepted manuscript online April 11, 2013/Article first published online May 12, 2013)

Rearrangements of the proto-oncogene *RET* are newly identified potential driver mutations in lung adenocarcinoma (LAD). However, the absence of cell lines harboring *RET* fusion genes has hampered the investigation of the biological relevance of RET and the development of RET-targeted therapy. Thus, we aimed to identify a *RET* fusion positive LAD cell line. Eleven LAD cell lines were screened for *RET* fusion transcripts by reverse transcription-polymerase chain reaction. The biological relevance of the *CCDC6-RET* gene products was assessed by cell growth, survival and phosphorylation of ERK1/2 and AKT with or without the suppression of RET expression using RNA interference. The efficacy of RET inhibitors was evaluated *in vitro* using a culture system and in an *in vivo* xenograft model. Expression of the *CCDC6-RET* fusion gene in LC-2/ad cells was demonstrated by the mRNA and protein levels, and the genomic break-point was confirmed by genomic DNA sequencing. Mutations in *KRAS* and *EGFR* were not observed in the LC-2/ad cells. CCDC6-RET was constitutively active, and the introduction of a siRNA targeting the *RET 3'* region decreased cell proliferation by downregulating RET and ERK1/2 phosphorylation. Moreover, treatment with RET-inhibitors, including vandetanib, reduced cell viability, which was accompanied by the downregulation of the AKT and ERK1/2 signaling pathways. Vandetanib exhibited anti-tumor effects in the xenograft model. Endogenously expressing CCDC6-RET contributed to cell growth. The inhibition of kinase activity could be an effective treatment strategy for LAD. LC-2/ad is a useful model for developing fusion RET-targeted therapy. (*Cancer Sci* 2013; 104: 896–903)

Lung cancer is the most common cause of cancer death worldwide.[1] The identification of oncogenic driver genes is to select the increasing number of small molecule inhibitors targeting these gene products.[2,3] In particular, in lung adenocarcinoma (LAD), the most dominant histological subtype of lung cancer, the application of kinase inhibitors for cases with specific gene alterations has been successful, that is, gefitinib and erlotinib for *EGFR* mutation-positive cases and crizotinib for *ALK* fusion-positive cases.[4–7] Furthermore, accumulating evidence has demonstrated somatic mutations and rearrangements of potential oncogenes, including *BRAF, ERBB2* and *ROS1*, in LAD.[8–10]

RET is one of the newest LAD driver genes.[11–15] *RET* gene is located on chromosome 10 and encodes a receptor tyrosine kinase,[16,17] and the oncogenic potential of this gene product has been suggested in several tumors, including thyroid cancer.[18–20] Recently, five independent groups identified aberrant fusion genes, *KIF5B-RET* and *CCDC6-RET* in clinical samples of LAD.[11–15] Ectopically expressed RET fusion products afforded NIH3T3 cells with anchorage-independent growth and tumorigenicity in nude mice.[11,14] Furthermore, KIF5B-RET-expressing H1299 cells exhibited growth factor-independent growth.[11] These findings strongly suggest the oncogenic activity of RET fusion products and also suggest the potential therapeutic efficacy of multi-kinase inhibitor targeting of RET using the abovementioned cells. However, LAD-derived cell lines harboring *RET* fusion genes had not been identified. Recently, Matsubara *et al.*[21] screened LAD cell lines that were sensitive to a RET inhibitor vandetanib and found a *CCDC6-RET* fusion gene-harboring cell line, LC-2/ad.

We have independently screened cell lines established from Japanese LAD samples by RT-PCR and found that LC-2/ad cells expressed the *CCDC6-RET* fusion gene product. We further examined whether LC-2/ad cells depend on RET fusion-mediated signaling. In addition, the antitumor effect of RET inhibitors in LC-2/ad cells was evaluated *in vitro* and *in vivo*.

Materials and Methods

Complete materials and methods were described in the supplementary information (Data S1. Materials and Methods).

Purchased materials. Cell lines were purchased from RIKEN Bio Resource Center, the Immuno-Biological Laboratories (Fujioka, Japan) and American Type Culture Collection. Procedures for western blotting was previously described.[22] Primary antibodies specific for RET and phospho-RET Tyr-905 were purchased from Epitomics (Burlingame, CA, USA) and Cell Signaling Technologies (Danvers, MA, USA), respectively. RET-targeting siRNA was purchased from Life Technologies (Carlsbad, CA, USA). Gefitinib, sunitinib malate and sorafenib were purchased from Santa Cruz Biotechnology (Dallas, TX, USA), Sigma-Aldrich (St. Louis, MO, USA) and Toronto Research Chemicals (Toronto, ON, Canada),

[10]To whom correspondence should be addressed.
E-mail: ktsuchih@east.ncc.go.jp
[11]These authors contributed equally to this work.

doi: 10.1111/cas.12175

respectively. Vandetanib, AZD6244 and BEZ235 were purchased from Selleck (Houston, TX, USA).

Multiplex RT-PCR. Reported *KIF5B/CCDC6-RET* fusion variants were detected by multiplex RT-PCR according to the procedures described elsewhere.[11,14]

Genomic DNA sequencing. LC-2/ad DNA was captured with custom hybridization probes targeting *CCDC6* intron 1 and *RET* whole gene (Agilent) followed by parallel sequencing on the MiSeq system (Illumina).

Real-time RT-PCR. Procedures for real-time RT-PCR was previously described.[22] The PCR primers used in the present study are shown in Table S1.

***In vivo* studies.** LC2/ad cells at 5.0×10^6 were subcutaneously inoculated to 8-week-old athymic nude mice (Clea Japan).[23] Vandetanib was administered once daily as a homogeneous suspension by oral gavage at a dosage of 50 mg/kg body weight.[24] The tumor volume was calculated as the product of a scaling factor ($\pi/6$) and the tumor length, width and height.[22] The study was approved by the Institutional Ethics Review Committee for animal experiments at the National Cancer Center.

Immunohistochemical analysis. The procedure for hematoxylin eosin staining and immunohistochemical (IHC) was previously described.[22,25]

Microarray analysis. Background information of clinical samples was described in a previous report.[26] The study was approved by the Institutional Review Boards of the National Cancer Center. Total RNA was analyzed using Affymetrix (Santa Clara, CA, USA) U133Plus2.0 arrays. The data were processed by the MAS5 algorithm, and the mean expression level of a total of 54 675 probes was adjusted to 1000 for each sample.

Results

Identification of the *CCDC6-RET* fusion gene in a Japanese LAD cell line. To identify *RET* fusion-derived mRNA expression in human LAD cell lines, all reported *KIF5B-RET* and *CCDC6-RET* gene products were screened by multiplex RT-PCR in 11 cell lines derived from Japanese patients. LC-2/ad cells were found to express *CCDC6-RET* mRNA at significantly higher levels, whereas the other cell lines did not exhibit any fusion gene products (Fig. 1a). The expressed fusion *RET* product was sequenced, and an in-frame fusion of *CCDC6* exon 1 and *RET* exon 12, which was identical to the previously reported *CCDC6-RET* fusion products, was identified (Fig. 1b).[14] We then identified a breakpoint of chromosome 10 by retrieving genomic DNA fragments, including the entire *RET* gene and intron 1 of *CCDC6*, by target capture system followed by parallel sequencing. The identified break-point between *CCDC6* intron 1 and *RET* exon 11 was confirmed by Sanger sequencing (Fig. 1b). Quantitative RT-PCR revealed that the expression of 3′ end of *RET* was increased comparable to that of *CCDC6*, whereas the transcript level of the 5′ end of *RET* was significantly lower (Fig. 1c). Consistent with the amount of transcript, western blotting using an antibody recognizing the C-terminus of RET isoform 2 detected a 60-kDa specific band equivalent to

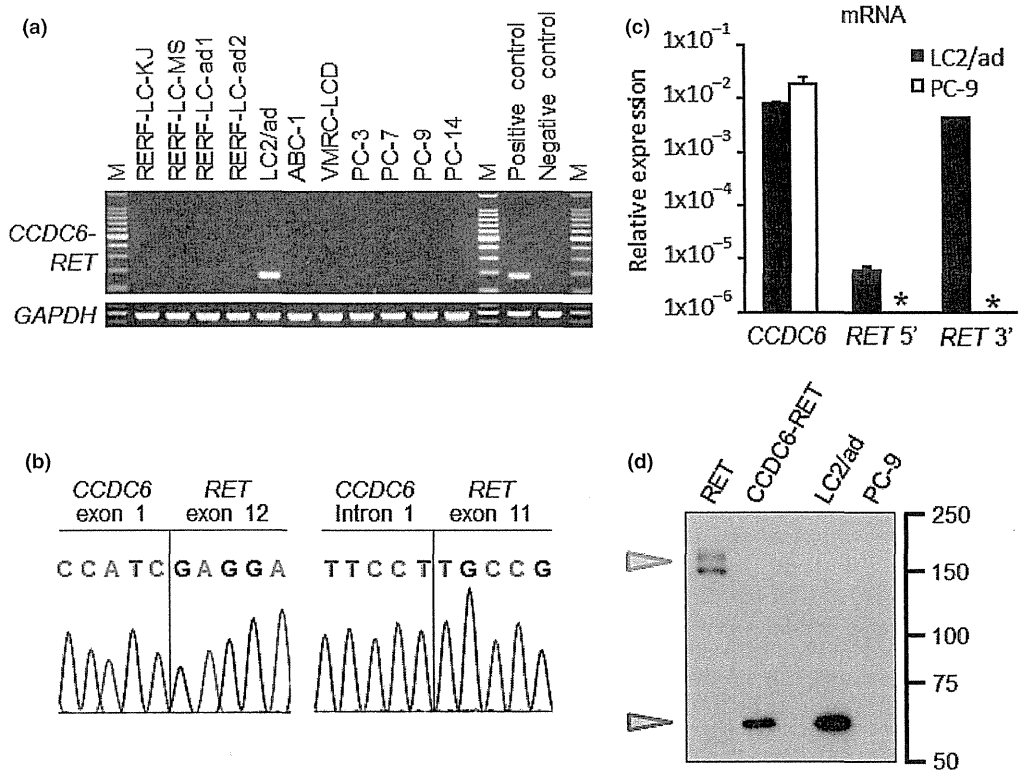

Fig. 1. Identification of the *CCDC6-RET* fusion gene. (a) Detection of *RET* fusion transcripts in lung adenocarcinoma (LAD) cell lines by multiplex reverse transcription-polymerase chain reaction (RT-PCR). (b) Sanger sequencing around the fusion point of the cDNA (left) and the breakpoint of the genomic DNA (right) of *CCDC6-RET* in LC-2/ad cells. (c) 3′ region-specific expression of *RET* mRNA in LC-2/ad cells. The 5′ or 3′ region of *RET* and *CCDC6* cDNA level was normalized to glyceraldehyde 3-phosphate dehydrogenase (*GAPDH*) expression. The data are shown as the mean ± standard deviation (SD) ($n = 3$). Asterisks indicate that mRNA expression were below the level of detection. (d) Specific expression of the CCDC6-RET fusion protein. Whole-cell lysates of LC2/ad and PC-9 cells and HEK293 cells transfected with wild-type RET (RET) or CCDC6-RET expression plasmids were subjected to western blot analysis to detect RET protein isoform 2. The LC-2/ad cells showed an approximately 60-kDa (red arrowhead) but not 170-kDa (blue arrowhead) band.

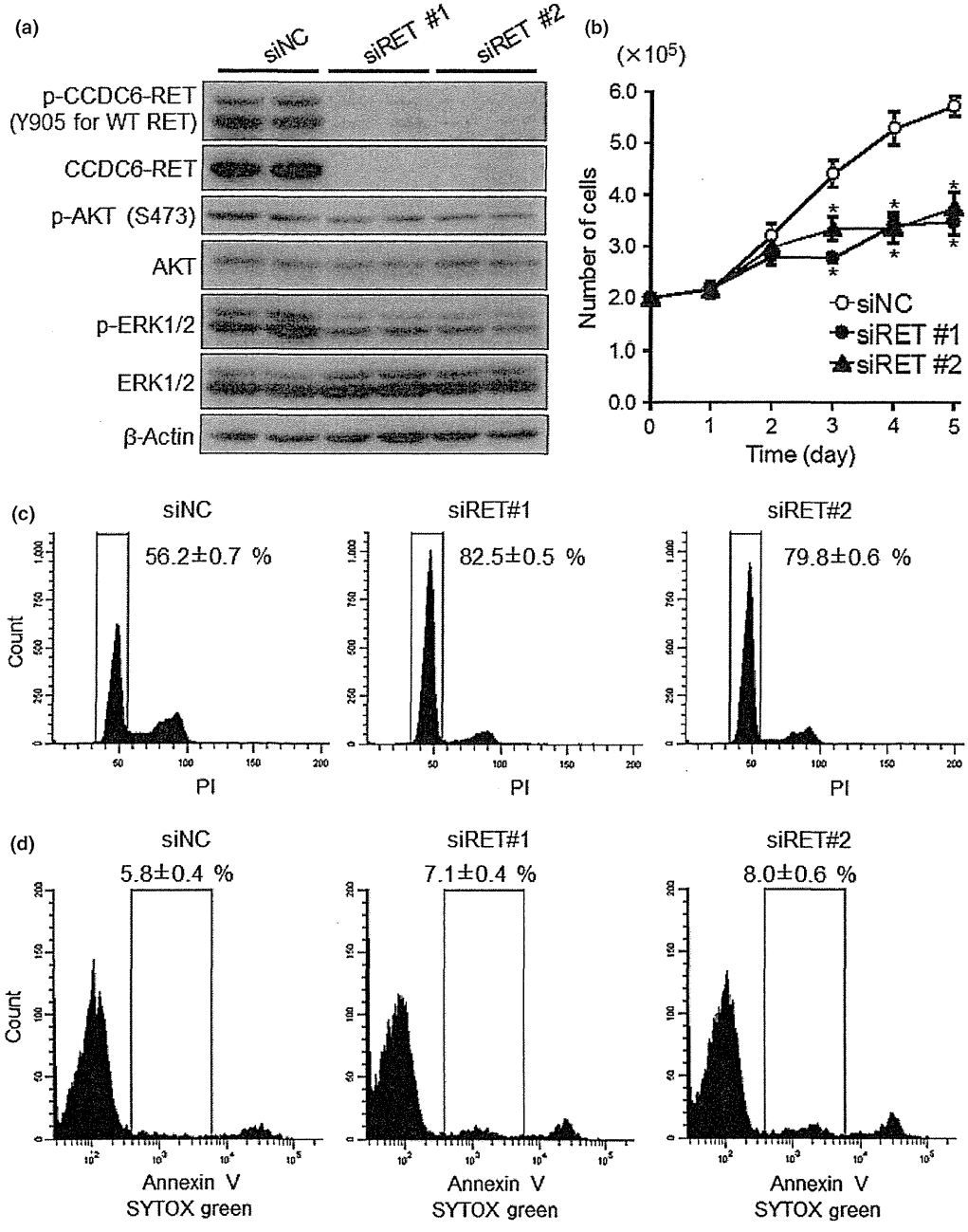

Fig. 2. Suppression of CCDC-RET expression by siRNA in LC-2/ad cells. (a) Western blot analysis of siRET-treated LC-2/ad cells. The siRNA transfected cell lysates were applied to the western blotting. (b) Involvement of RET suppression in cell growth inhibition. LC-2/ad cells transfected with siRNAs were incubated for the indicated times. The data are shown as the mean ± standard deviation (SD) ($n = 4$). *$P < 0.01$ (Student's *t*-test). (c,d) The DNA ploidy (c) and Annexin V-positive population (d) of siRET-transfected LC-2/ad cells. After 72 h of siRNA transfection, the cells were subjected to DNA ploidy analysis and Annexin V staining. The data are shown as the mean ± SD ($n = 4$).

the estimated size of the fusion protein composed of 503 amino acids (GeneBank BAM36435), whereas no significant signal was detected that approximated the size of wild-type RET, 170-kDa (Fig. 1d).[11] Taken together, we concluded that LC-2/ad cells express *CCDC6-RET* fusion gene products. *KRAS* exon 2 and *EGFR* exon 19 and 21 were examined by Sanger sequencing, but no obvious mutation was confirmed (Fig. S1).

CCDC6-RET-dependent ERK1/2 phosphorylation and the proliferation of LC-2/ad cells. We suppressed *RET* expression by RNAi to characterize the function of CCDC6-RET in LC-2/ad cells. For avoiding off-target siRNA effects, two different sequences of siRNA directed against the 3′ region of *RET* (siRET#1 and #2) and a nontargeting siRNA (siNC) were used. When compared to siNC, a significant reduction in mRNA expression was observed by quantitative RT-PCR detecting the 3′ end of the *RET* mRNA: 66.5% for siRET#1 and 94.2% for siRET#2 (Fig. S2). Western blot analyses also revealed significant decreases in the expression of CCDC6-RET protein (60-kDa) upon the introduction of siRET#1 and #2 compared to the control siNC in the LC-2/ad cells

doi: 10.1111/cas.12175

(Fig. 2a). To examine whether the downstream signaling pathway was altered by the introduction of siRNA, the phosphorylation of ERK1/2 and AKT was examined. The phospho-ERK1/2 signal was significantly decreased by the suppression of CCDC6-RET expression, whereas the decrease of AKT phosphorylation was marginal (Fig. 2a). The involvement of RET fusion in LC-2/ad cell proliferation was then examined. The number of live CCDC6-RET-suppressed cells decreased throughout the experiment, and the difference became significant at day 3 and thereafter (Fig. 2b). To address the growth suppression further, the cell cycle of the siRNA-treated cells were assessed by the DNA ploidy pattern. The LC-2/ad cells treated with siRET exhibited significant increases in the percent of cells arrested in the G1 phase relative to the cells treated with siNC (Fig. 2c). However, the apoptotic cells, as assessed by Annexin V positivity, was not significantly increased by the suppression of RET expression (Fig. 2d).

RET-dependent transcriptome profile in LC-2/ad cell. To characterize the transcriptome profile, which is regulated by CCDC6-RET and its downstream signaling pathway, siRET#2 and siNC treated LC-2/ad cells were subjected to genome-wide expression profiling using Affymetrix U133Plus2.0 arrays. A total of 243 genes, evaluated with 285 probes were selected as those preferentially suppressed by less than half in siRET-treated cells.As well, 566 genes with 661 probes were expressed more than twice in siRET-treated cells (Table S2 and Fig. S3). The *RET* gene itself (probe ID = 211421_s_at) showed the highest fold-difference of 19.6 between siNC- and siRET#2-treated cells. Following *RET*, previously identified Gene Ontology-annotated Ras-MAPK downstream genes like *DUSP6* was preferentially suppressed in the siRET-treated cells. In addition, cell cycle regulation-related genes like *EREG, CDC6, MCM10, MAD2L1, CHEK1* and *PLK4* were expressed <0.5-fold in siRET-treated cells (Table 1).

RET fusion gene screening of 300 consecutive surgically resected LAD samples identified one case of *CCDC6-RET* expressing LAD by RT-PCR and break-apart FISH (Tsuta *et al.*, 2012, unpublished data). We checked the expression level of potential CCDC6-RET-driven genes identified above in the clinical sample. Among 285 preferentially expressed probes, 81 probes were also upregulated more than twofold in the *CCDC6-RET* positive LAD tissue compared to the surrounding non-cancerous tissue (Table 1 and Table S2).

RET inhibitor-induced cell cycle arrest and apoptosis in LC-2/ad cells. The phosphorylation status of the tyrosine 905 residue of RET isoforms 2 and 4 was high in the LC-2/ad cells, regardless of the presence or absence of serum in the culture medium, whereas the total amount of RET isoform 2 was not significantly altered. Similarly, the phosphorylation status of AKT and ERK1/2 was high under serum-starved conditions, and the enhanced phosphorylation of these molecules was slight with serum stimulation, suggesting that the fusion RET kinase was constitutively active and activated its downstream signaling pathways (Fig. 3a).

Next, the effects of kinase inhibitors, which inhibit spectrum including RET were applied to evaluate their effects on the signaling pathways in the LC-2/ad cells. We treated the cells with RET inhibitors vandetanib, sunitinib and sorafenib at a final concentration of 10 μM, which was 10–30 times higher than the *in vitro* half maximal inhibitory concentration (IC_{50}) for RET kinase activity of each compound. Gefitinib, another small molecule inhibitor targeting EGFR but not RET,[13] was also examined. All the inhibitors except gefitinib significantly suppressed the phosphorylation of RET, AKT and ERK1/2. Although vandetanib, sunitinib and sorafenib equivalently suppressed RET phosphorylation, vandetanib most significantly suppressed the phosphorylation of ERK1/2 (Fig. 3a). The inhibitory effect of vandetanib on RET, AKT and ERK1/2 phosphorylation exhibited concentration dependency (Fig. 3b). Gefitinib significantly suppressed EGFR phosphorylation while total EGFR protein level was not altered. Meanwhile, gefitinib did not alter the phosphorylation status of AKT and ERK1/2 (Fig. 3a). Meanwhile, vandetanib suppressed EGFR as well as AKT and ERK1/2 in *EGFR*-mutant PC-9 cells (Fig. S4).

We further examined the effect of the above inhibitors on the growth of the LC-2/ad cells using the WST-8 assay. Consistent with the effects of the inhibitors on the RET signaling pathway, vandetanib suppressed cell growth most significantly (IC_{50} = 0.32 μM), followed by sunitinib and sorafenib, whereas gefitinib only exhibited an apparent suppression at its highest dose (Fig. 3c). However, the effects of these inhibitors on *KRAS*-mutant A549 cells were much lower (Fig. S5). Gefitinib and vandetanib, both of which inhibit EGFR, suppressed *EGFR*-mutant PC-9 cells, whereas sunitinib and sorafenib had less effect (Fig. S5). Evaluating the number of live cells by trypan blue staining under the treatment of several doses of

Table 1. Up- or downregulated genes associated with mitogen-activated protein kinase (MAPK) cascade or cell cycle

Gene symbol	Probe set ID	siNC/siRET	Tumor/Non-tumor
Upregulated			
RET	211421_s_at	19.63	19.52
	205879_x_at	3.76	5.03
	215771_x_at	2.37	4.72
DUSP6	208892_s_at	4.45	5.22
	208893_s_at	4.17	6.34
	208891_at	4.17	3.56
EREG	1569583_at	3.68	1.60
	205767_at	2.93	5.69
CDC6	203967_at	2.42	4.82
	203968_s_at	1.95	5.32
MCM10	220651_s_at	2.30	4.83
	223570_at	1.72	1.71
MAD2L1	203362_s_at	2.28	5.91
	1554768_a_at	1.91	4.34
CHEK1	205394_at	2.17	9.03
	205393_s_at	2.14	6.87
PLK4	204886_at	2.07	4.38
	204887_s_at	1.56	4.08
Downregulated			
MEF2C	209200_at	0.21	0.46
	209199_s_at	0.26	0.65
GAB1	214987_at	0.23	0.42
	229114_at	0.53	0.65
	225998_at	0.62	0.68
	226002_at	0.64	0.76
CDKN1C	216894_x_at	0.26	0.41
	213348_at	0.32	0.23
	213183_s_at	0.35	0.30
	219534_x_at	0.42	0.27
	213182_x_at	0.44	0.21
PTEN	233314_at	0.33	0.27
	225363_at	0.77	0.47
TIMP2	231579_s_at	0.34	0.33
	224560_at	0.37	0.27
ID2	201566_x_at	0.35	0.31
	201565_s_at	0.40	0.39
	213931_at	0.52	0.31
CCNL2	232274_at	0.35	0.42
	222999_s_at	0.79	0.52
RPS6KA2	212912_at	0.41	0.34
	204906_at	0.59	0.49

vandetanib suggested a dose-dependent suppression in the LC-2/ad cells. Furthermore, the number of cells treated with 0.5 and 1.0 μM vandetanib was apparently reduced to less than the starting amount, strongly suggesting that vandetanib induced both cell death and the suppression of cell proliferation (Fig. 3d). An assessment of the DNA ploidy revealed that vandetanib arrested the cell cycle in G1 phase in a dose-dependent manner (Fig. 3e), and an increased concentration of vandetanib induced an Annexin V-positive apoptotic cell population (Fig. 3f). The proapoptotic effect of vandetanib was confirmed by the detection of cleaved caspase-3 by western blotting (Fig. 3b). Meanwhile, 1.0 μM sunitinib and sorafenib induced cell cycle arrest but induction of apoptosis was marginal (Figs S6 and S7).

To further evaluate the contribution of Ras-ERK and AKT axes to cell survival, LC-2/ad cells were treated with MEK1/2 inhibitor AZD6244 or PI3K/mTOR inhibitor BEZ235. Cytotoxic effect of AKT-inhibiting BEZ235 was more than that of ERK-inhibiting AZD6244. However, both inhibitors did not completely reduce the cell survival even their maximal dose (Figs S8 and S9).

Anti-tumor effect of vandetanib in an LC-2/ad xenograft model. Subcutaneously transplanted LC-2/ad tumors exhibited typical adenocarcinoma morphology. These tumors were positive for SFTPA, Napsin A and carcinoembryonic antigen (CEA) but thyroid marker thyroglobulin negative using immunohistochemistry (IHC). Furthermore, using an antibody cross-reacting with both human and mouse RET protein, IHC revealed that RET was highly expressed specifically in the tumor cells but not in the interstitial cells (Fig. 4a). The overexpression of RET in these tumors was confirmed using quantitative RT-PCR and Western blotting. Similar to the results from cultured LC-2/ad cells, much more mRNA of the 3′ end of *RET* was detected than that of the 5′ end (Fig. 4b), and a specific band equivalent to the size of the CCDC6-RET fusion protein was detected (Fig. 4c). Vandetanib (50 mg/kg) was orally administrated to the mice harboring the LC-2/ad xenograft, and the daily administration of vandetanib significantly reduced the tumor size. Although the tumors were diminished at day 14 of the treatment, the body weight of the treated mice was not significantly reduced (Fig. 4d and Fig. S10). Sorafenib (30 mg/kg) and sunitinib (40 mg/kg) did not reduce the body weight, either (Fig. S10). Sorafenib reduced but not diminished the tumors at day14. Anti-tumor effect of sunitinib was not significant (Fig. S11).

Discussion

Previous reports suggest that the incidence of *RET*-fusion-positive cases in LAD is 1–2% and that these cases are concentrated in the *EGFR* mutation-, *KRAS* mutation-, and *ALK*-fusion-negative population.[10,27] To identify cell lines expressing endogenous *RET*-fusion genes, we selected 11 cell lines that were derived from pathologically identified Japanese LAD cases. Among them, activating EGFR mutations have been reported in PC-3 and PC-9 cells.[28] However, the mutation status of known driver genes of other cell lines was not well investigated. The LC-2/ad cells were originally derived from pleural effusion of LAD in a patient who had received combined chemotherapy (endoxan, Adriamycin, Cisplatin and mitomycin C)[23]; the cancer was diagnosed by cytological examination of the patient's sputum and pleural effusion. The original report indicated that the LC-2/ad cells were positive for an adenocarcinoma marker, cytokeratin 18.[23] In addition, we detected surfactant protein, an aspartate proteinase, Napsin A, and CEA expression in the xenograft tumor (Fig. 4a). These findings support the origin of LC-2/ad as lung adenocarcinoma. The modal chromosome number described in the original report was 53–56, though an apparent translocation between the chromosomes was not reported, consistent with the fact that the inversion of chromosome 10 was not obvious in the conventional chromosome counts.

The Sanger sequencing in this study and the whole-transcriptome sequencing (Tsuchihara, 2012, unpublished data) revealed no driver mutations of *KRAS*, *EGFR* and known genes other than the *CCDC6-RET* fusion in the LC-2/ad cells, highly suggesting that the CCDC6-RET fusion protein plays pivotal roles in the proliferation of these cells. The autophosphorylation of CCDC6-RET was clearly observed in a serum-independent manner, accompanied with a constitutive elevation of ERK1/2 phosphorylation. The suppression of CCDC6-RET expression induced a decrease in ERK1/2 phosphorylation, accompanied with a decrease in the expression of the genes that regulate the cell cycle. As a result, the CCDC6-RET-suppressed cells exhibited significant growth retardation.

Recently, a Japanese group independently reported the CCDC6-RET fusion in LC2/ad cells.[21] However, the efficacy of RET inhibitors to the RET and downstream pathways and *in vivo* anti-tumor effects have been partially described.[21] Vandetanib, sorafenib and sunitinib suppress the activities of multiple kinases, including RET, and have been approved for several cancers.[29–31] In *in vitro* analyses, these compounds effectively suppressed the phosphorylation of CCDC6-RET and suppressed proliferation and induced death in LC-2/ad cells. It should be noted that the IC_{50} value for the growth suppression of these compounds was equivalent to the dose suggested in a previous study using culture cells expressing ectopic *KIF5B-RET* cDNA.[13] These effects were most likely dependent on RET inhibition. Sunitinib and sorafenib did not affect PC-9 and A549 cells, which have activating mutations of *EGFR* and *KRAS*, respectively. Vandetanib presumably suppressed the growth of PC-9 cells, as EGFR is included in its inhibitory spectrum. Meanwhile, gefitinib, which targets EGFR but not RET, did not significantly suppress the growth of LC-2/ad cells. Interestingly, gefitinib did not alter the phosphorylation of AKT and ERK1/2 in LC-2/ad cells albeit equivalently suppressing EGFR phosphorylation as vandetanib. Although precise molecular mechanisms should be further examined, LC-2/ad cells might not depend on EGFR for transducing downstream signaling.

Vandetanib exhibited apparent anti-tumor effects in the xenograft model in this study. Recently, efficacy of vandetanib on thyroid cancer cells harboring *RET*-fusion gene was also reported.[32] These findings strongly suggest that RET inhibition is a plausible therapeutic strategy for RET-fusion-positive tumors.

We noticed a discrepancy between the effects of RNA interference and inhibitor treatment on RET. Though RET suppression/inhibition equivalently reduced the level of phosphorylated RET and induced cell cycle arrest, obvious apoptosis was not found in the cells treated with siRNA. A possible explanation is that CCDC6-RET is mainly involved in the RAS-ERK pathway to regulate cell proliferation, whereas the anti-apoptotic signaling pathway mediated by AKT could be regulated by other signaling molecules inhibited by the multi-kinase inhibitors. A recent study using a Drosophila *in vivo* screening system suggested that the antitumor effects and toxicity of RET inhibitors were dependent on the profile of the "off-target" inhibition of multiple kinases in addition to the specific inhibition of RET.[33] Further investigation elucidating the molecules and signaling pathways relevant to the cytotoxic effect of vandetanib in LC-2/ad cells is anticipated.

Whether LC-2/ad-based models adequately represent clinical *RET* fusion-positive LAD cases is another challenging question. Takeuchi stated that clinically identified *CCDC6-RET*-positive LAD exhibited a histologically cribriform pattern.[14]

doi: 10.1111/cas.12175

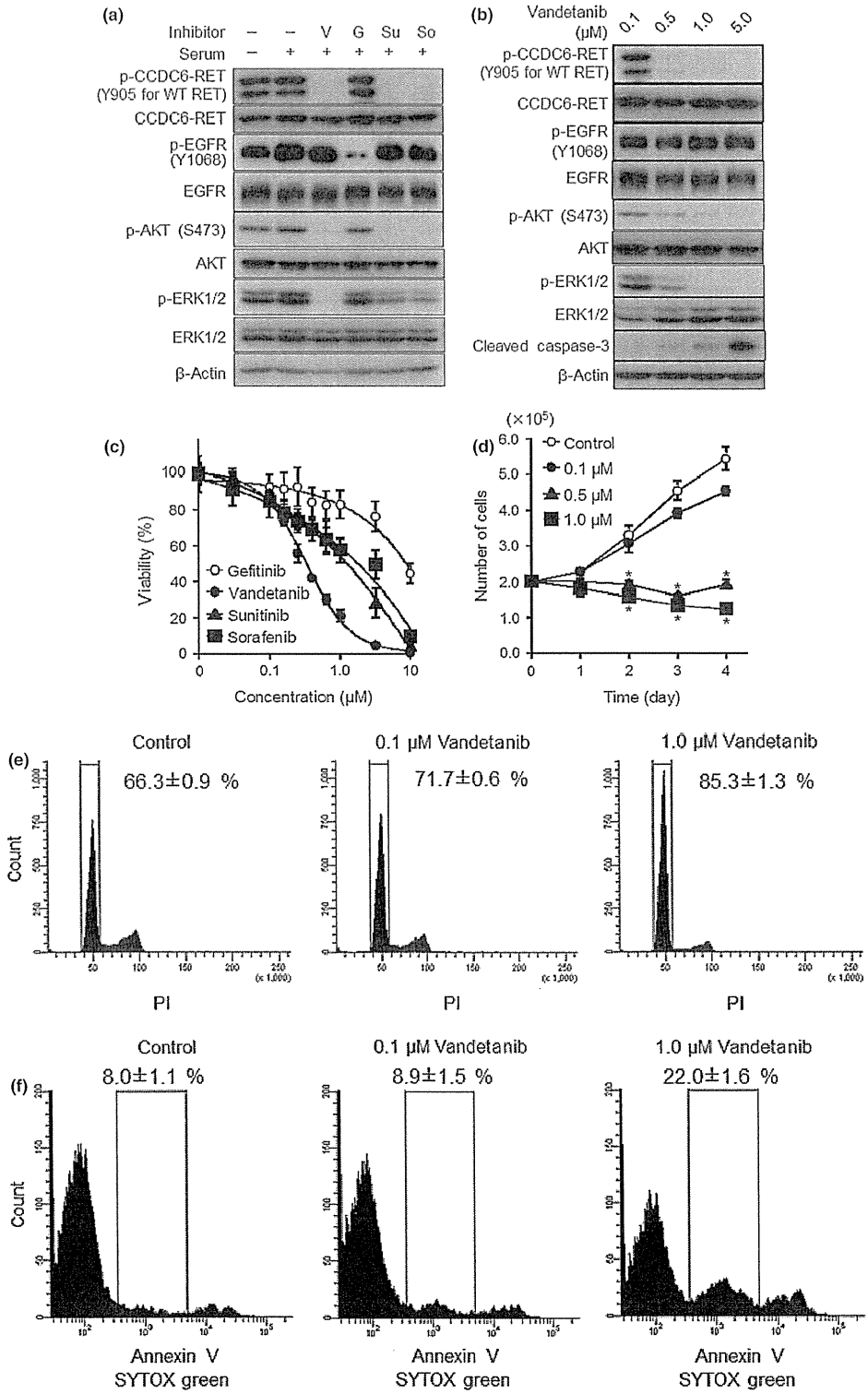

Fig. 3. Effect of RET inhibitors on LC-2/ad cells. (a) Western blot analysis of inhibitor-treated cells. The cells were incubated under serum-starved conditions for 22 h and treated with 1 μM of inhibitor or dimethylsulfoxide (DMSO) for 2 h. Prior to cell lysis, the cells were treated with 10% fetal bovine serum (FBS) for 10 min. Whole-cell lysates were subjected to western blot analysis to detect the indicated proteins. G, gefitinib; So, sorafenib; Su, sunitinib; V, vandetanib. (b) Dose-dependent effect of vandetanib. Cells were treated with the indicated concentration of vandetanib for 12 h, and western blotting was used to detect the indicated proteins. (c) WST-8 assay with kinase inhibitors. Cells were treated with the indicated inhibitors for 72 h, and the viability was assessed using the WST-8 assay. The data are shown as the mean ± standard deviation (SD) (n = 6). (d) Effect of vandetanib for growth inhibition. Cells were treated with vandetanib and incubated for the indicated time. The data are shown as the mean ± SD (n = 3). *P < 0.01 (Student's t test). (e,f) DNA ploidy (e) and Annexin V-positive population (f) of the cells treated with vandetanib for 48 h. The data are shown as the mean ± SD (n = 4).

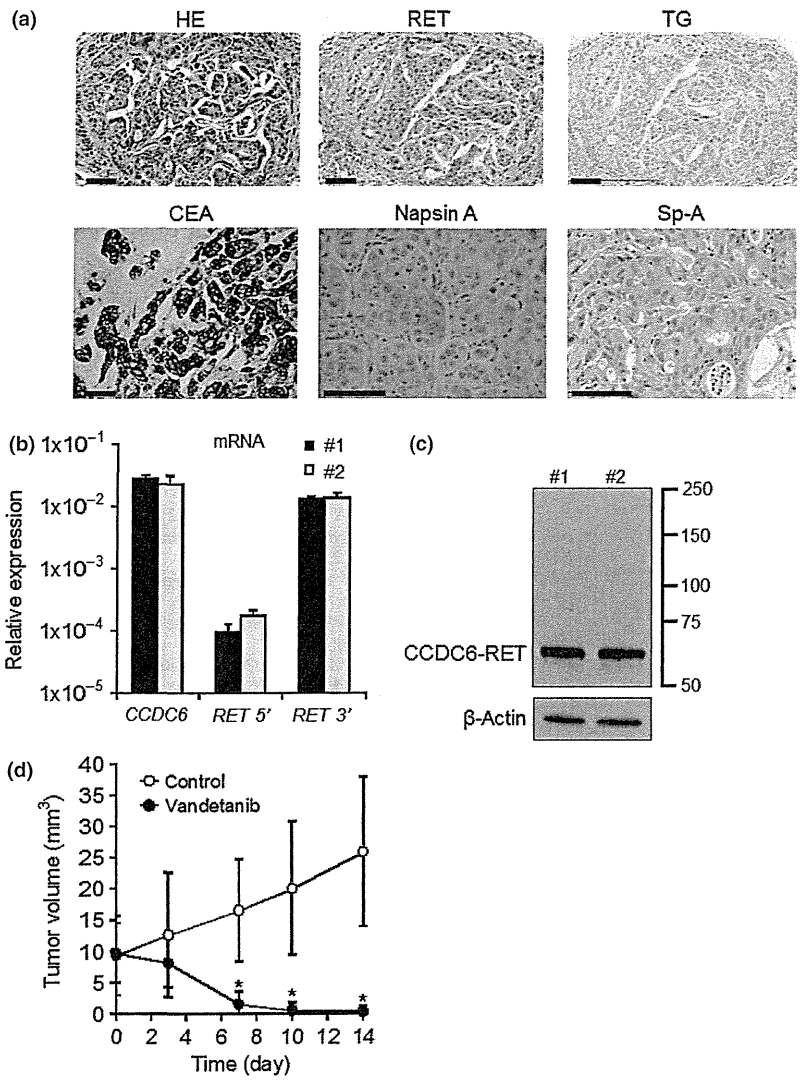

Fig. 4. Characterization of the LC-2/ad xenograft and anti-tumor effects of vandetanib. (a) Histological features of the xenograft. Hematoxylin and eosin staining and immunohistochemical staining with the indicated antibodies. Scale bars were 100 μm. Hematoxylin eosin (HE), RET, thyroglobulin (TG) and carcinoembryonic antigen (CEA) (×20); Napsin A and Sp-A (×40). (b) 3′ region-specific expression of *RET* mRNA in the xenograft. Total RNA extracted from tumors was subjected to real-time reverse transcription-polymerase chain reaction (RT-PCR) analysis with the primer sets designed for the 5′ or 3′ region of the *RET* and *CCDC6* cDNA. The data are shown as the mean ± standard deviation (SD) ($n = 3$). (c) Expression of the CCDC6-RET protein in mice xenografts. Whole-cell lysates of tumors were subjected to western blot analysis. (d) Anti-tumor effect of vandetanib *in vivo*. Vandetanib was administered once a day at a dosage of 50 mg/kg. The data are shown as the mean ± SD ($n = 9$). *$P < 0.01$ (control *vs* sorafenib; Student's *t* test).

Because the cribriform structure was presumably developed from normal alveolar architecture, this specific morphology was not observed in the subcutaneously transplanted LC-2/ad tumors. We assume that the comparison of the transcriptome profile between the LC-2/ad cells and clinically identified LAD tissue samples may provide clues. Approximately one-third of the genes suppressed by RNA interference directed at *RET* overlapped with the genes preferentially expressed in the clinical tumor sample. Because we have had only one example of paired data, it is difficult to estimate the similarity between the cell line and clinical samples. However, the above overlap appears promising, and we will continue to screen both cell lines and clinical samples to accumulate comprehensive data.

In this study, the screening of Japanese LAD cell lines was effective for the identification of *RET* fusion-positive cancer cells, representing a clinically rare subpopulation. LC-2/ad cells might be useful in the development of RET-targeted therapies, that is, new compound screening, clarifying the pharmacological mechanisms and investigating the mechanisms for acquired resistance.

Acknowledgments

We thank Drs Hiroki Sasaki and Kazuhiko Aoyagi and the National Cancer Center Research Core Facility for the microarray analyses. The Core Facility was supported by National Cancer Center Research and Development Fund (23-A-7). This work was supported by National Cancer Center Research and Development Fund (23-A-8, 15, 24-A-1) and JSPS KAKENHI Grant number 24300345.

Disclosure Statement

The authors have no conflict of interest.

References

1 Jemal A, Bray F, Center MM, Ferlay J, Ward E, Forman D. Global cancer statistics. *CA Cancer J Clin* 2011; **61**: 69–90.

2 Pao W, Girard N. New driver mutations in non-small-cell lung cancer. *Lancet Oncol* 2011; **12**: 175–80.

3 Pao W, Chmielecki J. Rational, biologically based treatment of EGFR-mutant non-small-cell lung cancer. *Nat Rev Cancer* 2010; **10**: 760–74.

doi: 10.1111/cas.12175